ON THE FIELD-INDUCED TRANSPORT OF MAGNETIC NANOPARTICLES IN INCOMPRESSIBLE FLOW: MODELING AND NUMERICS

G. GRÜN AND P. WEISS

Abstract. By methods from non-equilibrium thermodynamics, we derive a class of nonlinear pde-models to describe the motion of magnetizable nanoparticles suspended in incompressible carrier fluids under the influence of external magnetic fields. Our system of partial differential equations couples Navier-Stokes and magnetostatic equations to evolution equations for the magnetization field and the particle number density. In the second part of the paper, a fully discrete mixed finite-element scheme is introduced which is rigorously shown to be energy-stable. Finally, we present numerical simulations in the 2D-case which provide first information about the interaction of particle density, magnetization and magnetic field.

1. Introduction

Superparamagnetic nanoparticles suspended in incompressible carrier liquids may be transported in a controlled way by means of external magnetic fields. This effect has various technological and medical applications. Probably most prominent is magnetic drug targeting. Here, magnetic nanoparticles are supposed to carry drug molecules, which are adhered to their surfaces, through the vascular system to precisely defined locations in the human body where they are needed, e.g., for tumor therapy. Another - more recent application - is related to molecular communication systems. Here, magnetic nanoparticles are used as message carriers in fluidic communication systems which are of such small size that communication based on electromagnetic waves can no longer be used (cf. [21,38,39]). Here, magnetic fields are expected to accelerate the transport of the magnetic nanoparticles used as message carriers and this way to sharpen signals by diminishing diffusive effects.

In this article, we use principles of non-equilibrium thermodynamics to derive a new system of partial differential equations for such processes, coupling Navier-Stokes equations and a convection-diffusion equation for the particle density to an evolution equation for the magnetization and to the magnetostatic equations. In the second part of the paper, we will propose a fully discrete finite-element scheme for this new model and establish stability estimates. The scheme has been implemented in the two-dimensional setting - first numerical simulations will be presented in the last section.

Date: October 14, 2019.

2010 *Mathematics Subject Classification.* 35Q35; 65M60.

Key words and phrases. Ferrohydrodynamics, magnetic nanoparticles, magnetization, system of partial differential equations, energy stable finite element scheme.

Before giving more details about the outline of the paper, let us comment on our modeling assumptions. We assume the nanoparticles under consideration to be superparamagnetic. This means that their magnetization changes randomly under the influence of temperature. Hence, in absence of external magnetic fields their magnetization is expected to decay to zero on average. As soon as an external field is switched on, the particles get easily magnetized and attracted by the magnetic field. In general, we expect

- the particles to be spherical with identical mass and size,
- their contribution to the gross momentum of the fluidic system to be negligible,
- particle-to-particle interactions, like agglomeration phenomena or anisotropic behaviour, not to occur and
- induced fields, like magnetization or the so called stray field, not to influence the applied external field $\mathbf{h}_a$.

Since the magnetization of superparamagnetic nanoparticles is such sensitive with respect to presence or absence of external magnetic fields, modeling approaches based on Landau-Lifshitz-Gilbert-equations (see, e.g. [9, 20, 23, 25, 26]) of micromagnetism seem not to be adequate. Indeed, these approaches assume the modulus of magnetization to be constant in space and time which is in strong contrast to the superparamagnetic behaviour described before.

In the literature liquids carrying magnetic nanoparticles are often labeled "ferrofluids", cf. [29]. In the field of ferrohydrodynamics mainly two lines of research can be distinguished so far. The first school is concerned with phenomena for which the particle distribution can be assumed to be homogeneous in space (and consequently constant in time). For those ferrofluids, pde-models have been derived by Shliomis [36] and Rosensweig [35]. Both models couple evolution equations for momentum and magnetization to Maxwell's equations or to their simplifications from magnetostatics. Rosensweig takes in addition an evolution equation for the angular momentum of the fluid into account. In a series of papers, Amirat and Hamdache [1–6] developed a mathematical existence theory in the framework of the Shliomis model. Just recently, Nochetto, Salgado and Tomas [28] proposed numerical schemes for the Rosensweig model. In a second paper, they [27] considered two-phase flow with one ferrofluid involved to model the famous Rosensweig instability [34], and they provided a convergence proof in a simplified setting. All of these publications have in common that there are no pathways suggested how to deal with non-homogeneous, non-steady particle densities.

In a second line of research, mathematical models have been suggested and investigated for the transport of magnetic nanoparticles with particle densities varying in space and time. These models have in common that evolution equations for the magnetization are not considered separately. Instead, authors assume the magnetization to be given explicitly as a function of particle density and magnetic field. Polevikov and Tobiska [32] were interested in a steady-state diffusion problem for particles in a ferrofluid. Most recently, Himmelsbach, Neuss-Radu and Neuß [19] proposed a new model featuring an evolution equation for the particle density coupled to the magnetostatic equations and assuming the macroscopic flow field to be given. In the radial symmetric case they show existence and uniqueness of solutions and provide numerical simulations, too.

Inspired by the work of Nochetto et al. [27, 28], in Section 2 we use Onsager's variational principle to derive a thermodynamically consistent model for the transport of magnetic nanoparticles in liquids. Here are the ingredients of our modeling approach. Starting from the total energy of the system - consisting of the magnetic field energy, Zeeman-type energies, the kinetic energy of the carrier liquid and a mixture energy - we combine generic evolution equations (with at this stage unspecified flux and coupling terms) for momentum and particle density with a Shliomis-type equation for magnetization and with the magnetostatic equations to determine a closed evolutionary system for flow field, magnetic field, magnetization and particle density.

In Section 3, we propose a numerical scheme based on a fully discrete formulation of this model with mixed finite elements - using - similarly as in [27] - in particular non-conforming elements for the magnetization. By a novel duality argument, it will nevertheless be possible to give a meaning to divergence and curl of the magnetization in the discrete setting. We expect this kind of higher regularity to be useful to obtain convergence results - which are, however, beyond the scope of this paper. Moreover, we present a discrete energy estimate which is consistent with the choice of total energy mentioned above.

The scheme has been implemented in the 2D-setting - in Section 4 we present some characteristic simulations. As a proof of concept, they show that the magnetization field is strongly coupled to the support of the superparamagnetic particles - and such details like, how streamlines of the magnetic field are influenced by the magnetization, become clearly visible.

We finish the introduction with some remarks on notation. We use the usual notation for Lebesgue and Sobolev spaces as well as for derivatives with respect to space and time. We write Ω for the fluidic domain and consider a larger domain Ω' containing Ω where the magnetic field $\mathbf{h}$ lives. Vectors and tensor fields are denoted in bold face, and

$$H^1_{t0}(\Omega)^d := \{\mathbf{N} \in H^1(\Omega)^d | \mathbf{N} \times \boldsymbol{\nu}|_{\partial\Omega} = 0\}$$

is defined as in [10]. Physical quantities will be introduced in Section 2 and in Subsection 3.1 the notation used for the numerical analysis will be explained.

2. Derivation of the model

We are going to derive a ferrohydrodynamics model by Onsager's variational principle [30, 31] featuring the hydrodynamic variables $\mathbf{u}, p$, the particle density c and the magnetic variables $\mathbf{m}, \mathbf{h}$. As usually, we assume the magnetic field $\mathbf{h}$ to be given as the sum of the external given field $\mathbf{h}_a$ and the so called stray or demagnetizing field $\mathbf{h}_d$. We also consider two different domains Ω, Ω', where $\Omega \subset \Omega'$ is the fluid domain and where the magnetic field will be defined on the larger domain Ω'. As sketched in Figure 2.1, the stray field usually acts demagnetizing on the magnetic material inside Ω. As indicated in Figure 2.1, we will impose boundary conditions on $\partial\Omega'$ and transmission conditions, cf. [12], on $\partial\Omega$. Denoting the jump across $\partial\Omega$ by $[\cdot]$, the latter read

$$\begin{aligned} [\mathbf{b}] \cdot \boldsymbol{\nu} &= 0, \\ [\mathbf{h}] \times \boldsymbol{\nu} &= 0, \end{aligned} \tag{2.1}$$

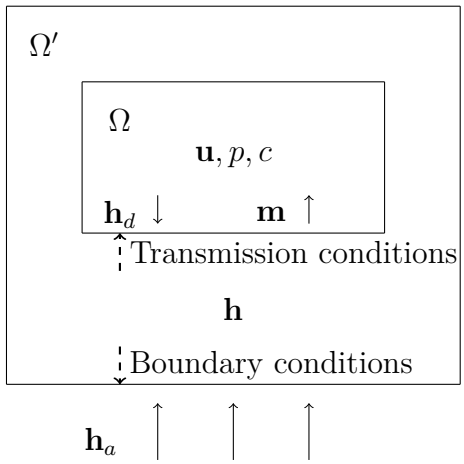

FIGURE 2.1. Sketch of the experimental setup.

where $\boldsymbol{\nu}$ is the outer unit normal to $\partial\Omega$ and the magnetic flux density is defined by

$$\mathbf{b} = \mu_0(\mathbf{h} + \mathbf{m}).$$

We assume a quasi-stationary evolution of the external magnetic field - hence it satisfies

$$\operatorname{div} \mathbf{h}_a = 0, \tag{2.2}$$

$$\operatorname{curl} \mathbf{h}_a = 0, \tag{2.3}$$

$$\mathbf{h}_a \in H^1([0,T]; H^2(\Omega')). \tag{2.4}$$

We start from generic evolution equations for the momentum and particle densities

$$\rho_0 \mathbf{u}_t + \rho_0(\mathbf{u}\cdot\nabla)\mathbf{u} + \nabla p - \operatorname{div}(\mathbf{T}) = \mathbf{k}, \tag{2.5}$$

$$\operatorname{div} \mathbf{u} = 0, \tag{2.6}$$

$$c_t + \mathbf{u}\cdot\nabla c + \operatorname{div}(\mathbf{J}) = 0 \tag{2.7}$$

in $\Omega \times (0,T)$, with the fluxes $\mathbf{J}, \mathbf{T}$ and the force density $\mathbf{k}$ to be determined later on. For simplicity, we add

$$\mathbf{u} = 0, \tag{2.8}$$

$$\mathbf{J}\cdot\mathbf{n} = 0, \tag{2.9}$$

as boundary conditions on $\partial\Omega \times [0,T]$. For the magnetic field, we use the magneto-static equations

$$\operatorname{div} \mathbf{b} = 0, \tag{2.10}$$

$$\operatorname{curl} \mathbf{h} = 0, \tag{2.11}$$

assuming free currents to be negligible. Note that introducing the potential R associated with the field $\mathbf{h}$,

$$\nabla R = \mathbf{h}, \tag{2.12}$$

(2.10) becomes

$$-\Delta R = \operatorname{div} \mathbf{m} \qquad \text{in } \Omega \times (0,T), \tag{2.13}$$

$$-\Delta R = 0 \qquad \text{in } (\Omega' \setminus \overline{\Omega}) \times (0,T). \tag{2.14}$$

The magnetization $\mathbf{m}$ is obtained via a derivation in the spirit of Shliomis [36] - in particular, we suppose

$$\mathbf{m} = \tilde{\chi}(c)\tilde{\mathbf{m}},$$

where $\tilde{\mathbf{m}}$ is the magnetic moment per particle, c the particle number density and $\tilde{\chi}$ is a not necessarily linear function (depending on the parameter regime) with the dimension of a particle number density. Magnetic nanoparticles have only a few magnetic domains or even just one single magnetic domain. We assume their structure to be simple enough to approximate the particle as single subdomain particle. Also, we assume all particles to be identical and to have the magnetic moment m_0 and volume V_0. The alignment of dilute magnetic dipoles in magnetic fields is disturbed by thermal fluctuation. For given magnetic field $\mathbf{h}$ and particle density c, the equilibrium magnetization $\mathbf{m}_{\text{eq}}$ can be described by the Langevin formula [24]

$$\begin{aligned} L(x) &= \coth x - \tfrac{1}{x}, \\ \mathbf{m}_{\text{eq}} &= \tilde{\chi}(c) m_0 L(\xi|\mathbf{h}|)\frac{\mathbf{h}}{|\mathbf{h}|}, \end{aligned}$$

which follows from Boltzmann statistics. Here, $\xi|\mathbf{h}| := \frac{\mu_0 m_0 |\mathbf{h}|}{k_B T}$ describes the ratio between the energy of a single magnetic dipole in a magnetic field $\mathbf{h}$ with magnetic moment m_0 and the thermal fluctuation energy at temperature T, where k_B is Boltzmann's constant. For a more detailed view on this formula see [19] - note that we view the Langevin formula in terms of magnetization instead of magnetic moments, see also [36]. For small values of $\xi|\mathbf{h}|$, some authors use the linearization with respect to $\mathbf{h}$,

$$\mathbf{m}_{\text{eq}} \approx \tilde{\chi}(c)\frac{\mu_0 m_0 M}{3k_B T}\mathbf{h} =: \chi(c)\mathbf{h}, \tag{2.15}$$

which we use for proof of concept numerics in Section 4 for simplification. The scalar value $\chi(c)$ is called susceptibility and describes to which extent the particles align parallel to the magnetic field. Note that depending on the parameter regime, χ not necessarily has to be a linear function, but in the linear case we have

$$\chi_{\text{lin}}(c) := \chi' c := \frac{\mu_0 m_0^2}{3k_B T}\, c, \tag{2.16}$$

which resembles the usual formula, which is also used e.g. in [19]. In the analysis-part of the present paper, however, we do not use only such a linearization as we prefer $\mathbf{m}_{\text{eq}}$ to stay bounded with respect to $\mathbf{h}$, hence

$$\mathbf{m}_{\text{eq}} = \chi(c,\mathbf{h})\mathbf{h} := \left(\tilde{\chi}(c) m_0 \frac{L(\xi|\mathbf{h}|)}{|\mathbf{h}|}\right)\mathbf{h}. \tag{2.17}$$

Note that $|\mathbf{m}_{\text{eq}}| \leq M\tilde{\chi}(c)$, but also in the linearized case (2.15), which only admits the estimate $|\mathbf{m}_{\text{eq}}| \leq \text{const.} \cdot \tilde{\chi}(c)|\mathbf{h}|$, an analogous energy estimate as in Theorem 3.1 can be obtained, see Remark 3.3.

Based on the formula for $\mathbf{m}_{\text{eq}}$, Shliomis [36] introduced an evolution equation for the magnetization that takes convection and rotation experienced by the magnetic particles into account. The alignment of magnetic particles exposed to a magnetic field depends on

Brown and Néel relaxation. We assume that both processes are described by one common relaxation time, e.g.

$$\frac{1}{\tau_{\text{rel}}} = \frac{1}{\tau_{\text{Brown}}} + \frac{1}{\tau_{\text{Néel}}},$$

see [36]. Following the same strategy as in [36] and considering diffusion as in [37], we make the ansatz

$$\frac{D'}{Dt}\mathbf{m} - \sigma\Delta\mathbf{m} = -\frac{1}{\tau_{\text{rel}}}(\mathbf{m} - \chi(c,\mathbf{h})\mathbf{h}),$$

where $\frac{D'}{Dt}$ is the material time derivative in a local coordinate system where the particles are assumed to be quiescent. Following the argumentation in [36] and assuming the magnetic particles' angular momentum to coincide with the angular momentum of the fluid, one gets

$$\frac{D'}{Dt}\mathbf{m} = \mathbf{m}_t + (\mathbf{v}\cdot\nabla)\mathbf{m} - \mathbf{w}\times\mathbf{m},$$

where $\mathbf{v}$ and $\mathbf{w}$ are the convection velocity and local angular momentum of the fluid medium, respectively. We approximate, as usual, $\mathbf{w} \approx \frac{1}{2}\operatorname{curl}\mathbf{u}$ and add the contribution of the flux to the convection velocity $\mathbf{v}$. This yields

$$\mathbf{m}_t + \operatorname{div}(\mathbf{m}\otimes(\mathbf{u} + \tfrac{\mathbf{J}}{c})) = \frac{1}{2}\operatorname{curl}\mathbf{u}\times\mathbf{m} - \frac{1}{\tau_{\text{rel}}}(\mathbf{m} - \chi(c,\mathbf{h})\mathbf{h}) + \sigma\Delta\mathbf{m}, \tag{2.18}$$

in $\Omega\times(0,T)$. Note that the term $\mathbf{u} + \frac{\mathbf{J}}{c}$ formally captures the velocity with which the particles are transported. Hence, the second term in (2.18) guarantees that particles and magnetization are transported with the same drift velocity.

To fix boundary conditions, we assume the stray field's contribution to the total field to be negligible at $\partial\Omega'$. From the transmission conditions (2.1), we infer

$$[\nabla R + \mathbf{m}] = 0 \qquad \text{on } \partial\Omega\times[0,T], \tag{2.19}$$

$$\nabla R\cdot\boldsymbol{\nu} = \mathbf{h}_a\cdot\boldsymbol{\nu} \qquad \text{on } \partial\Omega'\times[0,T], \tag{2.20}$$

where $\mathbf{m}$ will be extended by 0 to $\Omega'\setminus\Omega$. Following the strategies in [1], we supplement the magnetization equation with the boundary conditions

$$\operatorname{curl}\mathbf{m}\times\boldsymbol{\nu} = 0, \tag{2.21}$$

$$\operatorname{div}\mathbf{m} = 0, \tag{2.22}$$

on $\partial\Omega\times[0,T]$. For $\mathbf{u}, c, \mathbf{m}$, initial conditions

$$\mathbf{u}(\cdot,0) = \mathbf{u}^0, \tag{2.23}$$

$$c(\cdot,0) = c^0, \tag{2.24}$$

$$\mathbf{m}(\cdot,0) = \mathbf{m}^0, \tag{2.25}$$

on Ω will be posed as well.

Let us discuss the (total) physical energy of the system. We introduce the kinetic energy

$$\frac{\rho_0}{2}\int_\Omega |\mathbf{u}|^2\ dx,$$

the particle's mixture energy

$$D\int_\Omega g(c)\ dx, \quad D\in\mathbb{R}^+,$$

with $g(c)=c\log c-c$, see e.g. [8, section 2.4], and the magnetic energy. The energy of the magnetic field is classically given by $\frac{1}{2}\int_{\Omega'}\mathbf{b}\cdot\mathbf{h}\ dx$. To capture further possible magnetic contributions to the total energy, we consider the interaction of the magnetizable particles with the field as well as the fact that the particles' magnetization decays in absence of (external) magnetic fields. The former may be described by Zeeman-type terms [20] which are proportional to $-\mathbf{m}\cdot\mathbf{h}$, for the latter the term $|\mathbf{m}|^2$ is a reasonable ansatz. As all this terms can be written as a superposition of terms like $|\mathbf{h}|^2, \mathbf{h}_a\cdot\mathbf{m}, \mathbf{h}_d\cdot\mathbf{m}$ and $|\mathbf{m}|^2$, we use the generic magnetic energy

$$\begin{aligned}\mathcal{E}_{\text{mag}} := \alpha_0\frac{\mu_0}{2}\int_{\Omega'}(|\mathbf{h}|^2+\mathbf{h}\cdot\mathbf{m})\ dx - \alpha_1\frac{\mu_0}{2}\int_\Omega \mathbf{h}_d\cdot\mathbf{m}\ dx \\ - \alpha_2\frac{\mu_0}{2}\int_\Omega \mathbf{h}_a\cdot\mathbf{m}\ dx + \alpha_3\frac{\mu_0}{2}\int_\Omega |\mathbf{m}|^2\ dx,\end{aligned} \tag{2.26}$$

with $\alpha_i, i=0,...,3$, being nonnegative parameters. In this formulation, coercivity of the magnetic energy with respect to $\mathbf{h}$ and $\mathbf{m}$ is not immediately obvious. To shed light on this issue, let us consider the weak formulation of the equation $\operatorname{div}\mathbf{b}=0$, taking also the boundary conditions (2.19),(2.20) into account. Let $\mathbf{m}$ be extended by zero to $\Omega'\setminus\Omega$. We multiply the equation by a test function $S\in H^1(\Omega')$, integrate by parts on Ω and $\Omega'\setminus\Omega$ separately and sum up. We get for arbitrary $S\in H^1(\Omega')$

$$\begin{aligned}0=\frac{1}{\mu_0}\int_{\Omega'}\operatorname{div}\mathbf{b}S\ dx &= \frac{1}{\mu_0}\int_{\Omega'}\mathbf{b}\cdot\nabla S\ dx - \frac{1}{\mu_0}\int_{\partial\Omega}[\mathbf{b}]\cdot\boldsymbol{\nu}S\ d\sigma - \frac{1}{\mu_0}\int_{\partial\Omega'}\mathbf{b}\cdot\boldsymbol{\nu}S\ d\sigma \\ &= \frac{1}{\mu_0}\int_{\Omega'}\mathbf{b}\cdot\nabla S\ dx - \int_{\partial\Omega'}\mathbf{h}_a\cdot\boldsymbol{\nu}S\ d\sigma \\ &= \frac{1}{\mu_0}\int_{\Omega'}\mathbf{b}\cdot\nabla S\ dx - \int_{\Omega'}\mathbf{h}_a\cdot\nabla S\ dx,\end{aligned}$$

where in the last two steps we used the boundary conditions (2.19),(2.20) and $\operatorname{div}\mathbf{h}_a=0$. Rewriting this formulation yields

$$\int_{\Omega'}\nabla R\cdot\nabla S\ dx = \int_{\Omega'}\mathbf{h}_a\cdot\nabla S\ dx - \int_\Omega \mathbf{m}\cdot\nabla S\ dx. \tag{2.27}$$

For completeness, we mention the following straightforward consequence of (2.27),

$$\int_{\Omega'}\nabla R_t\cdot\nabla S\ dx = \int_{\Omega'}(\mathbf{h}_a)_t\cdot\nabla S\ dx - \int_\Omega \mathbf{m}_t\cdot\nabla S\ dx \tag{2.28}$$

for all $S\in H^1(\Omega')$. Let R_a denote the potential of the external magnetic field, $\mathbf{h}_a=\nabla R_a$. Testing (2.27) by R and by $(R-R_a)$, respectively, one readily obtains the following

equivalent formulation of (2.26)

$$\begin{aligned}\mathcal{E}_{\text{mag}} = \alpha_0 \frac{\mu_0}{2} \int_{\Omega'} \mathbf{h}_a \cdot \mathbf{h} \, dx + \alpha_1 \frac{\mu_0}{2} \int_{\Omega'} |\mathbf{h} - \mathbf{h}_a|^2 \, dx \\ - \alpha_2 \frac{\mu_0}{2} \int_{\Omega} \mathbf{h}_a \cdot \mathbf{m} \, dx + \alpha_3 \frac{\mu_0}{2} \int_{\Omega} |\mathbf{m}|^2 \, dx.\end{aligned} \tag{2.29}$$

In this version, coercivity with respect to $\mathbf{h}$ and $\mathbf{m}$ is obvious.

Putting everything together, for the total energy we obtain

$$\begin{aligned}\mathcal{E} := \frac{\rho_0}{2} \int_{\Omega} |\mathbf{u}|^2 \, dx + D \int_{\Omega} g(c) \, dx \\ + \alpha_0 \frac{\mu_0}{2} \int_{\Omega'} (|\mathbf{h}|^2 + \mathbf{h} \cdot \mathbf{m}) \, dx - \alpha_1 \frac{\mu_0}{2} \int_{\Omega} \mathbf{h}_d \cdot \mathbf{m} \, dx \\ - \alpha_2 \frac{\mu_0}{2} \int_{\Omega} \mathbf{h}_a \cdot \mathbf{m} \, dx + \alpha_3 \frac{\mu_0}{2} \int_{\Omega} |\mathbf{m}|^2 \, dx.\end{aligned}$$

Let us proceed with determining the fluxes $\mathbf{J}, \mathbf{T}$ as well as the force density $\mathbf{k}$ via Onsager's variational principle, cf. [11, 15, 33]. Using equations (2.5)-(2.9) and integration by parts, the time-derivative of the first two terms in $\mathcal{E}$ is readily obtained as

$$\begin{aligned}\partial_t \left(\frac{\rho_0}{2} \int_{\Omega} |\mathbf{u}|^2 \, dx + D \int_{\Omega} g(c) \, dx \right) \\ = - \int_{\Omega} \mathbf{T} : \nabla \mathbf{u} \, dx + \int_{\Omega} \mathbf{k} \cdot \mathbf{u} \, dx + D \int_{\Omega} \nabla g'(c) \cdot \mathbf{J} \, dx,\end{aligned} \tag{2.30}$$

where we used $\operatorname{div} \mathbf{u} = 0$ and integration by parts twice to deduce

$$\int_{\Omega} c \nabla g'(c) \cdot \mathbf{u} \, dx = - \int_{\Omega} \nabla (g'(c)) \cdot \mathbf{u} \, dx = 0.$$

The magnetic terms require some preparations. Let us first discuss the role of the individual terms in the magnetic energy. Each term will produce a term of the form $\int_{\Omega} \mathbf{m}_t \cdot \boldsymbol{\phi} \, dx$ where $\boldsymbol{\phi}$ can be $\mathbf{h}_a, \mathbf{h}_d$ or $\mathbf{m}$. Recalling $\nabla R = \mathbf{h}$,

$$\begin{aligned}\partial_t \int_{\Omega'} (|\mathbf{h}|^2 + \mathbf{h} \cdot \mathbf{m}) \, dx &\overset{(2.27)}{=} \partial_t \int_{\Omega'} \mathbf{h}_a \cdot \mathbf{h} \, dx \\ &= \int_{\Omega'} (\mathbf{h}_a)_t \cdot \mathbf{h} \, dx + \int_{\Omega'} \mathbf{h}_a \cdot \mathbf{h}_t \, dx \\ &\overset{(2.28)}{=} \int_{\Omega'} (\mathbf{h}_a)_t \cdot \mathbf{h} \, dx + \int_{\Omega'} (\mathbf{h}_a)_t \cdot \mathbf{h}_a \, dx - \int_{\Omega'} \mathbf{m}_t \cdot \mathbf{h}_a \, dx,\end{aligned}$$

$$\begin{aligned}-\partial_t \int_{\Omega} \mathbf{h}_d \cdot \mathbf{m} \, dx &\overset{(2.27)}{=} \partial_t \int_{\Omega'} |\mathbf{h}_d|^2 \, dx \\ &= 2 \int_{\Omega'} (\mathbf{h}_d)_t \cdot \mathbf{h}_d \, dx \\ &\overset{(2.28)}{=} -2 \int_{\Omega} \mathbf{m}_t \cdot \mathbf{h}_d \, dx\end{aligned}$$

$$-\partial_t \int_\Omega \mathbf{h}_a \cdot \mathbf{m}\ dx = -\int_\Omega (\mathbf{h}_a)_t \cdot \mathbf{m}\ dx - \int_\Omega \mathbf{m}_t \cdot \mathbf{h}_a\ dx$$

$$\partial_t \int_\Omega |\mathbf{m}|^2\ dx = 2\int_\Omega \mathbf{m}_t \cdot \mathbf{m}\ dx.$$

Altogether we need to discuss the term

$$-\frac{\mu_0}{2}\int_\Omega \mathbf{m}_t \cdot ((\alpha_0+\alpha_2)\mathbf{h}_a + 2\alpha_1\mathbf{h}_d - 2\alpha_3\mathbf{m})\ dx. \tag{2.31}$$

Observe that the remaining terms contain time derivatives only of $\mathbf{h}_a$. Therefore, they are not relevant with respect to model derivation by Onsager's principle. Let us simplify

$$\begin{aligned}(\alpha_0+\alpha_2)\mathbf{h}_a + 2\alpha_1\mathbf{h}_d - 2\alpha_3\mathbf{m}\\ &= 2\alpha_1\mathbf{h}\ +\ (\alpha_0+\alpha_2-2\alpha_1)\mathbf{h}_a\ -\ 2\alpha_3\mathbf{m}\\ &=: 2\alpha_1\mathbf{h} + \beta\mathbf{h}_a - 2\alpha_3\mathbf{m}\\ &=: \hat{\mathbf{h}} - 2\alpha_3\mathbf{m} =: \hat{\mathbf{b}}.\end{aligned} \tag{2.32}$$

Inspired by (2.31), let us derive a formula for $\mu_0\int_\Omega \mathbf{m}_t\cdot(-\alpha_1\mathbf{h}+\alpha_3\mathbf{m})\ dx$. For this, we use (2.18) as well as the zero boundary conditions for $\mathbf{u}, \operatorname{div}\mathbf{m}, \operatorname{curl}\mathbf{m}\times\boldsymbol{\nu}, \mathbf{J}\cdot\boldsymbol{\nu}$ on $\partial\Omega$, the fact that $(\mathbf{a}\times\mathbf{b})\cdot\mathbf{c}$ is an alternating trilinearform, $\operatorname{curl}\mathbf{h}=0$ and the representation $\Delta = -\operatorname{curl}\operatorname{curl} + \nabla\operatorname{div}$. Note that

$$\int_\Omega \operatorname{div}(\mathbf{m}\otimes\mathbf{v})\cdot\mathbf{w}\ dx = -\int_\Omega (\mathbf{v}\cdot\nabla)\mathbf{w}\cdot\mathbf{m}\ dx$$

when $\mathbf{v}\cdot\boldsymbol{\nu}=0$ on $\partial\Omega$ and that

$$\int_\Omega \operatorname{curl}\mathbf{a}\cdot\mathbf{b}\ dx = \int_\Omega \mathbf{a}\operatorname{curl}\mathbf{b}\ dx - \int_{\partial\Omega}(\mathbf{a}\times\boldsymbol{\nu})\cdot\mathbf{b}\ d\sigma. \tag{2.33}$$

This gives

$$\begin{aligned}
&\mu_0\int_\Omega \mathbf{m}_t\cdot(-\alpha_1\mathbf{h}+\alpha_3\mathbf{m})\ dx\\
&= -\alpha_1\mu_0\int_\Omega(\mathbf{u}\cdot\nabla)\mathbf{h}\cdot\mathbf{m}\ dx + \alpha_3\mu_0\int_\Omega(\mathbf{u}\cdot\nabla)\mathbf{m}\cdot\mathbf{m}\ dx\\
&\quad -\alpha_1\mu_0\int_\Omega(\tfrac{\mathbf{J}}{c}\cdot\nabla)\mathbf{h}\cdot\mathbf{m}\ dx + \alpha_3\mu_0\int_\Omega(\tfrac{\mathbf{J}}{c}\cdot\nabla)\mathbf{m}\cdot\mathbf{m}\ dx\\
&\quad -\frac{\alpha_1\mu_0}{2}\int_\Omega \operatorname{curl}\mathbf{u}\times\mathbf{m}\cdot\mathbf{h}\ dx + \frac{\alpha_3\mu_0}{2}\int_\Omega \operatorname{curl}\mathbf{u}\times\mathbf{m}\cdot\mathbf{m}\ dx\\
&\quad +\frac{\alpha_1\mu_0}{\tau_{\mathrm{rel}}}\int_\Omega \mathbf{m}\cdot\mathbf{h}\ dx - \frac{\alpha_3\mu_0}{\tau_{\mathrm{rel}}}\int_\Omega |\mathbf{m}|^2\ dx\\
&\quad -\frac{\alpha_1\mu_0}{\tau_{\mathrm{rel}}}\int_\Omega \chi(c,\mathbf{h})|\mathbf{h}|^2\ dx + \frac{\alpha_3\mu_0}{\tau_{\mathrm{rel}}}\int_\Omega \chi(c,\mathbf{h})\mathbf{h}\cdot\mathbf{m}\ dx\\
&\quad +\alpha_1\mu_0\sigma\int_\Omega \operatorname{curl}\operatorname{curl}\mathbf{m}\cdot\mathbf{h}\ dx - \alpha_1\mu_0\sigma\int_\Omega \nabla\operatorname{div}\mathbf{m}\cdot\mathbf{h}\ dx\\
&\quad -\alpha_3\mu_0\sigma\int_\Omega \operatorname{curl}\operatorname{curl}\mathbf{m}\cdot\mathbf{m}\ dx + \alpha_3\mu_0\sigma\int_\Omega \nabla\operatorname{div}\mathbf{m}\cdot\mathbf{m}\ dx
\end{aligned}$$

$$
\begin{aligned}
= & -\alpha_1\mu_0\int_\Omega(\mathbf{u}\cdot\nabla)\mathbf{h}\cdot\mathbf{m}\;dx-\alpha_1\mu_0\int_\Omega(\tfrac{\mathbf{J}}{c}\cdot\nabla)\mathbf{h}\cdot\mathbf{m}\;dx\\
&+\alpha_3\mu_0\int_\Omega(\tfrac{\mathbf{J}}{c}\cdot\nabla)\mathbf{m}\cdot\mathbf{m}\;dx-\frac{\alpha_1\mu_0}{2}\int_\Omega\operatorname{curl}(\mathbf{m}\times\mathbf{h})\cdot\mathbf{u}\;dx\\
&+\frac{\alpha_1\mu_0}{\tau_{\mathrm{rel}}}\int_\Omega\mathbf{m}\cdot\mathbf{h}\;dx-\frac{\alpha_3\mu_0}{\tau_{\mathrm{rel}}}\int_\Omega|\mathbf{m}|^2\;dx-\frac{\alpha_1\mu_0}{\tau_{\mathrm{rel}}}\int_\Omega\chi(c,\mathbf{h})|\mathbf{h}|^2\;dx\\
&+\frac{\alpha_3\mu_0}{\tau_{\mathrm{rel}}}\int_\Omega\chi(c,\mathbf{h})\mathbf{h}\cdot\mathbf{m}\;dx+\alpha_1\mu_0\sigma\int_\Omega\operatorname{div}\mathbf{m}\cdot\operatorname{div}\mathbf{h}\;dx\\
&-\alpha_3\mu_0\sigma\int_\Omega|\operatorname{curl}\mathbf{m}|^2\;dx-\alpha_3\mu_0\sigma\int_\Omega|\operatorname{div}\mathbf{m}|^2\;dx.
\end{aligned}
$$

The magnetostatic equation and its weak formulation (2.27) admit some simplification. We have

$$
\alpha_1\mu_0\sigma\int_\Omega\operatorname{div}\mathbf{m}\cdot\operatorname{div}\mathbf{h}\;dx=-\alpha_1\mu_0\sigma\int_{\Omega'\setminus\partial\Omega}|\operatorname{div}\mathbf{h}|^2\;dx
$$

and

$$
\frac{\alpha_1\mu_0}{\tau_{\mathrm{rel}}}\int_\Omega\mathbf{m}\cdot\mathbf{h}\;dx=\frac{\alpha_1\mu_0}{\tau_{\mathrm{rel}}}\int_{\Omega'}\mathbf{h}_a\cdot\mathbf{h}\;dx-\frac{\alpha_1\mu_0}{\tau_{\mathrm{rel}}}\int_{\Omega'}|\mathbf{h}|^2\;dx.
$$

Introducing the abbreviations

$$
\begin{aligned}
\mathcal{D}_{\mathrm{mag}}:=&\frac{\alpha_3\mu_0}{\tau_{\mathrm{rel}}}\int_\Omega|\mathbf{m}|^2\;dx+\frac{\alpha_1\mu_0}{\tau_{\mathrm{rel}}}\int_\Omega\chi(c,\mathbf{h})|\mathbf{h}|^2\;dx\\
&+\frac{\alpha_1\mu_0}{\tau_{\mathrm{rel}}}\int_{\Omega'}|\mathbf{h}|^2\;dx+\alpha_3\mu_0\sigma\int_\Omega|\operatorname{curl}\mathbf{m}|^2\;dx\\
&+\alpha_3\mu_0\sigma\int_\Omega|\operatorname{div}\mathbf{m}|^2\;dx+\alpha_1\mu_0\sigma\int_{\Omega'\setminus\partial\Omega}|\operatorname{div}\mathbf{h}|^2\;dx,\\
\mathbf{k}^{\mathbf{h}}_{\mathrm{mag}}:=&-\alpha_1\mu_0\int_\Omega(\mathbf{u}\cdot\nabla)\mathbf{h}\cdot\mathbf{m}\;dx-\frac{\alpha_1\mu_0}{2}\int_\Omega\operatorname{curl}(\mathbf{m}\times\mathbf{h})\cdot\mathbf{u}\;dx,\\
\mathcal{F}^{\mathbf{h}}_{\mathrm{mag}}:=&\frac{\alpha_0\mu_0}{2}\int_{\Omega'}(\mathbf{h}_a)_t\cdot\mathbf{h}_a\;dx+\frac{\alpha_0\mu_0}{2}\int_{\Omega'}(\mathbf{h}_a)_t\cdot\mathbf{h}\;dx\\
&-\frac{\alpha_2\mu_0}{2}\int_\Omega(\mathbf{h}_a)_t\cdot\mathbf{m}\;dx+\frac{\alpha_1\mu_0}{\tau_{\mathrm{rel}}}\int_{\Omega'}\mathbf{h}_a\cdot\mathbf{h}\;dx
\end{aligned}
$$

we arrive at

$$
\begin{aligned}
\partial_t\mathcal{E}_{\mathrm{mag}}=\mathbf{k}^{\mathbf{h}}_{\mathrm{mag}}+\mathcal{F}^{\mathbf{h}}_{\mathrm{mag}}-\mathcal{D}_{\mathrm{mag}}+&\frac{\alpha_3\mu_0}{\tau_{\mathrm{rel}}}\int_\Omega\chi(c,\mathbf{h})\mathbf{h}\cdot\mathbf{m}\;dx-\frac{\beta\mu_0}{2}\int_\Omega\mathbf{m}_t\cdot\mathbf{h}_a\;dx\\
&-\alpha_1\mu_0\int_\Omega(\tfrac{\mathbf{J}}{c}\cdot\nabla)\mathbf{h}\cdot\mathbf{m}\;dx+\alpha_3\mu_0\int_\Omega(\tfrac{\mathbf{J}}{c}\cdot\nabla)\mathbf{m}\cdot\mathbf{m}\;dx.
\end{aligned}
$$

Using $\operatorname{div}\mathbf{h}_a=0$, $\operatorname{curl}\mathbf{h}_a=0$, we analogously end up with

$$
\begin{aligned}
&-\frac{\beta\mu_0}{2}\int_\Omega\mathbf{m}_t\cdot\mathbf{h}_a\;dx\\
&\quad=\mathbf{k}^{\mathbf{h}_a}_{\mathrm{mag}}+\frac{\beta\mu_0}{2\tau_{\mathrm{rel}}}\int_\Omega\mathbf{m}\cdot\mathbf{h}_a\;dx-\frac{\beta\mu_0}{2\tau_{\mathrm{rel}}}\int_\Omega\chi(c,\mathbf{h})\mathbf{h}\cdot\mathbf{h}_a\;dx-\frac{\beta\mu_0}{2}\int_\Omega(\tfrac{\mathbf{J}}{c}\cdot\nabla)\mathbf{h}_a\cdot\mathbf{m}\;dx,
\end{aligned}
$$

where

$$\mathbf{k}_{\text{mag}}^{\mathbf{h}_a} := -\frac{\beta\mu_0}{2}\int_\Omega (\mathbf{u}\cdot\nabla)\mathbf{h}_a\cdot\mathbf{m}\,dx - \frac{\beta\mu_0}{4}\int_\Omega \operatorname{curl}(\mathbf{m}\times\mathbf{h}_a)\cdot\mathbf{u}\,dx.$$

Summing up,

$$\begin{aligned}\partial_t\mathcal{E} = &-\int_\Omega \mathbf{T}:\nabla\mathbf{u}\,dx + \int_\Omega \mathbf{k}\cdot\mathbf{u}\,dx + D\int_\Omega \nabla g'(c)\cdot\mathbf{J}\,dx\\ &+\mathbf{k}_{\text{mag}}^{\mathbf{h}} + \mathbf{k}_{\text{mag}}^{\mathbf{h}_a} - \mathcal{D}_{\text{mag}} + \mathcal{F}_{\text{mag}}^{\mathbf{h}}\\ &\quad -\alpha_1\mu_0\int_\Omega (\tfrac{\mathbf{J}}{c}\cdot\nabla)\mathbf{h}\cdot\mathbf{m}\,dx + \alpha_3\mu_0\int_\Omega (\tfrac{\mathbf{J}}{c}\cdot\nabla)\mathbf{m}\cdot\mathbf{m}\,dx\\ &\quad +\frac{\alpha_3\mu_0}{\tau_{\text{rel}}}\int_\Omega \chi(c,\mathbf{h})\mathbf{h}\cdot\mathbf{m}\,dx + \frac{\beta\mu_0}{2\tau_{\text{rel}}}\int_\Omega \mathbf{m}\cdot\mathbf{h}_a\,dx\\ &\quad -\frac{\beta\mu_0}{2\tau_{\text{rel}}}\int_\Omega \chi(c,\mathbf{h})\mathbf{h}\cdot\mathbf{h}_a\,dx - \frac{\beta\mu_0}{2}\int_\Omega (\tfrac{\mathbf{J}}{c}\cdot\nabla)\mathbf{h}_a\cdot\mathbf{m}\,dx.\end{aligned} \tag{2.34}$$

Now we define our dissipation functional as a function of the unknown quantities,

$$\mathcal{D}(\mathbf{T},\mathbf{J}) := \int_\Omega \frac{|\mathbf{T}|^2}{4\eta}\,dx + \int_\Omega \frac{|\mathbf{J}|^2}{2f_2(c)K}\,dx,$$

where K is the mobility of the particles and $f_2(c)$ describes the propagation behavior, possibly regularized at $c=0$. Together with (2.34), the (symmetric) stress tensor $\mathbf{T}$ and the flux $\mathbf{J}$ are determined by

$$\begin{aligned}\mathbf{T} &= 2\eta\mathbf{D}\mathbf{u},\\ \mathbf{J} &= -KDf_2(c)\nabla g'(c) + K\mu_0\frac{f_2(c)}{c}(\nabla\overbrace{(\alpha_1\mathbf{h}+\tfrac{\beta}{2}\mathbf{h}_a-\alpha_3\mathbf{m})}^{\hat{\mathbf{b}}/2})^T\mathbf{m},\end{aligned} \tag{2.35}$$

respectively. For the force density, we get

$$\mathbf{k} := \mu_0(\nabla(\alpha_1\mathbf{h}+\tfrac{\beta}{2}\mathbf{h}_a))^T\mathbf{m} + \frac{\mu_0}{2}\operatorname{curl}(\mathbf{m}\times\underbrace{(\alpha_1\mathbf{h}+\tfrac{\beta}{2}\mathbf{h}_a)}_{\hat{\mathbf{h}}/2}). \tag{2.36}$$

Note that the term $(\nabla\hat{\mathbf{h}})^T\mathbf{m} = (\mathbf{m}\cdot\nabla)\hat{\mathbf{h}}$ - due to $\operatorname{curl}\hat{\mathbf{h}} = 0$ - represents the Kelvin force and $(\nabla\mathbf{m})^T\mathbf{m} = \frac{1}{2}\nabla|\mathbf{m}|^2$ can be seen as contribution to the particles' chemical potential. We continue by introducing the effective diffusive flow velocity field

$$\mathbf{V}_{\text{part}} := \frac{\mathbf{J}}{c}. \tag{2.37}$$

The final system reads

$$\begin{aligned}&\rho_0\mathbf{u}_t + \rho_0(\mathbf{u}\cdot\nabla)\mathbf{u} + \nabla p - \operatorname{div}(2\eta\mathbf{D}\mathbf{u})\\ &\qquad = \mu_0(\mathbf{m}\cdot\nabla)(\alpha_1\mathbf{h}+\tfrac{\beta}{2}\mathbf{h}_a) + \frac{\mu_0}{2}\operatorname{curl}(\mathbf{m}\times(\alpha_1\mathbf{h}+\tfrac{\beta}{2}\mathbf{h}_a)),\end{aligned} \tag{2.38a}$$

$$\operatorname{div}\mathbf{u} = 0, \tag{2.38b}$$

$$c_t + \mathbf{u}\cdot\nabla c + \operatorname{div}(c\mathbf{V}_{\text{part}}) = 0, \tag{2.38c}$$

$$\mathbf{V}_{\text{part}} = -KD\frac{f_2(c)}{c}\nabla g'(c) + K\mu_0\frac{f_2(c)}{c^2}(\nabla(\alpha_1\mathbf{h}+\tfrac{\beta}{2}\mathbf{h}_a-\alpha_3\mathbf{m}))^T\mathbf{m}, \tag{2.38d}$$

$$-\Delta R = \operatorname{div}(\chi_\Omega\mathbf{m}), \tag{2.38e}$$

$$\mathbf{m}_t + \operatorname{div}(\mathbf{m} \otimes (\mathbf{u} + \mathbf{V}_{\text{part}})) - \sigma \Delta \mathbf{m} = \frac{1}{2} \operatorname{curl} \mathbf{u} \times \mathbf{m} - \frac{1}{\tau_{\text{rel}}} (\mathbf{m} - \chi(c, \mathbf{h})\mathbf{h}), \quad (2.38\text{f})$$

If for the mixture energy the classical entropic term $g(c) = c \log c - c$ is used, two choices for $f_2(c)$ are most prominent. First, $f_2(c) \sim c$ entails a linear diffusion term in the evolution equation for c while $f_2(c) \sim c^2$ makes the effective particle velocity field $\mathbf{V}_{\text{part}}$ linear in c and causes finite speed of propagation of the nano-particles, too [17].

3. A stable numerical scheme

3.1. **Formulation of the scheme.** Let $\mathcal{T}_h(\Omega')$ and $\mathcal{T}_h(\Omega)$ be families of open simplices in $\mathbb{R}^d$, such that

$$\overline{\Omega'} = \bigcup_{K \in \mathcal{T}_h(\Omega')} \overline{K}, \qquad \overline{\Omega} = \bigcup_{K \in \mathcal{T}_h(\Omega)} \overline{K},$$
$$\mathcal{T}_h(\Omega) \subset \mathcal{T}_h(\Omega').$$

Let

$$\begin{aligned} \mathcal{D}_k(\overline{\Omega'}) := \{ f : \overline{\Omega'} \to \mathbb{R} | \forall K \in \mathcal{T}_h(\Omega') : \forall \mathbf{x} \in K : \\ f(\mathbf{x})|_K \;=\; \sum_{|\alpha_K| \le k} a_{\alpha_K} \mathbf{x}^{\alpha_K}|_K \;\text{ for multi-indices } \alpha_K \in \mathbb{N}^d \\ \text{and associated numbers } a_{\alpha_K} \in \mathbb{R} \} \end{aligned}$$

denote the space of piecewise polynomials of order less or equal to k and

$$\mathcal{D}_k^{\text{mean}}(\overline{\Omega'}) := \Big\{ f \in \mathcal{D}_k(\overline{\Omega'}) \Big| \int_{\Omega'} f \; dx = 0 \Big\}$$

the space of those functions with mean value zero. We will also consider subspaces of continuous functions denoted by

$$\mathcal{P}_k(\overline{\Omega'}) := \mathcal{D}_k(\overline{\Omega'}) \cap C(\overline{\Omega'}),$$
$$\mathcal{P}_k^{\text{mean}}(\overline{\Omega'}) := \mathcal{D}_k^{\text{mean}}(\overline{\Omega'}) \cap C(\overline{\Omega'}).$$

On Ω, corresponding function spaces are defined analogously. Let

$$\begin{aligned} &\mathcal{U}_h = \mathcal{P}_2(\overline{\Omega})^d \cap H_0^1(\Omega)^d, && \Psi_h = \mathcal{P}_1(\overline{\Omega})^d, && \mathcal{M}_h = \mathcal{D}_1(\overline{\Omega})^d, \\ &\mathcal{P}_h = \mathcal{P}_1^{\text{mean}}(\overline{\Omega}), && \mathcal{C}_h = \mathcal{P}_1(\overline{\Omega}), && \mathcal{R}_h = \mathcal{P}_2^{\text{mean}}(\overline{\Omega'}), \end{aligned}$$

denote the finite element spaces associated with the unknowns $\mathbf{u}, \mathbf{J}, \mathbf{m}, p, c, R$, respectively. Note that the Taylor-Hood element [18], we have chosen for the Navier-Stokes equations, satisfies the inf-sup condition and that the discrete magnetization may be discontinuous. Note that the choice of $\mathcal{M}_h$ has been inspired by [27]. We decompose the time interval into subintervals

$$[0, T] = \bigcup_{k=1,\ldots,n_T} [t^{k-1}, t^k],$$

where for simplicity $t^k = t^{k-1} + \tau$, $\tau > 0$ and $t^0 = 0$. For functions f defined on space-time domain $\Omega \times [0, T]$ or $\Omega' \times [0, T]$, we abbreviate

$$f^k(\cdot) := f(\cdot, t^k).$$

Let

$$\mathcal{I}^d_{h,2} : C(\overline{\Omega})^d \to \mathcal{P}_2(\overline{\Omega})^d, \qquad \mathcal{I}_{h,1} : C(\overline{\Omega}) \to \mathcal{P}_1(\overline{\Omega}),$$

denote the nodal interpolation operators. Similarly, let

$$\hat{\mathcal{I}}^d_{h,1} : \{\mathbf{f} : \Omega \to \mathbb{R}^d |\ \mathbf{f}|_K \in C(\overline{K})^d\ \forall K \in \mathcal{T}_h(\Omega)\} \to \mathcal{D}_1(\overline{\Omega})^d,$$
$$\hat{\mathcal{I}}_{h,1} : \{f : \Omega \to \mathbb{R} |\ f|_K \in C(\overline{K})\ \forall K \in \mathcal{T}_h(\Omega)\} \to \mathcal{D}_1(\overline{\Omega})$$

be the nodal interpolation operators, where interpolation is done individually for all simplices using the corresponding nodal values of the continuous extensions on each simplex. We also need to define discrete approximations of compositions, e.g. $g_s'(c)$. Given $u \in \mathcal{D}(\overline{\Omega})$ and $f \in C(\mathbb{R})$, we denote the nodal interpolation of the composite function $f(u)$ by

$$f_h(u) := \hat{\mathcal{I}}_{h,1}(f(u)) \in \mathcal{D}_1(\overline{\Omega}).$$

Correspondingly, $f_h^k = f_h(u(\cdot, t^k))$ stands for evaluation at the time instant t^k. Similarly,

$$(\mathbf{h}_a)_h^k := \mathcal{I}^d_{h,1}(\mathbf{h}_a(\cdot, t^k)).$$

We introduce a regularised entropy given by

$$g_s(c) := \begin{cases} \frac{c^2}{2s} + (\log s - 1)c - \frac{s}{2} & \text{for } c \le s, \\ c \log c - c & \text{for } c > s. \end{cases} \tag{3.1}$$

Obviously,

$$g_s'(c) = \begin{cases} \frac{c}{s} + \log s - 1 & \text{for } c \le s, \\ \log c & \text{for } c > s, \end{cases}$$

$$g_s''(c) = \begin{cases} \frac{1}{s} & \text{for } c \le s, \\ \frac{1}{c} & \text{for } c > s. \end{cases}$$

Hence, g_s is convex. In particular, we choose $s \le e$, implying $(\log s - 1) \le 0$. Susceptibility needs to be regularised as well. We enforce nonnegativity and for large values of c only sublinear growth. More precisely, for given $r > 0$ consider

$$\chi_r(c, \mathbf{h}) := m_0 \frac{L(\xi|\mathbf{h}|)}{|\mathbf{h}|} \begin{cases} \max(0, c) & \text{for } c\frac{m_0\xi}{3} < r, \\ \sqrt{c - \frac{3r}{m_0\xi} + \frac{1}{4}} + \frac{3r}{m_0\xi} - \frac{1}{2} & \text{else.} \end{cases} \tag{3.2}$$

This definition admits the estimates

$$0 \le \chi_r(c, \mathbf{h}) \le K_1 + K_2\sqrt{c}, \tag{3.3}$$

$$0 \le |\chi_r(c, \mathbf{h})\mathbf{h}| \le K_1 + K_2\sqrt{c} \tag{3.4}$$

for some constants $K_1, K_2 > 0$ (depending on r). To deal with gradients of discontinuous finite element functions consistency terms are necessary. The set of inner faces on Ω is defined by

$$\mathcal{F}_{\text{int}} = \left(\bigcup_{K \in \mathcal{T}(\Omega)} \partial K \right) \setminus \partial\Omega$$

and each face $E \in \mathcal{F}_{\text{int}}$ has one arbitrarily fixed unit normal $\boldsymbol{\nu}^E$. Then $\boldsymbol{\nu}^{\mathcal{F}_{\text{int}}} : \mathcal{F}_{\text{int}} \to \mathbb{R}^d$ is just the function, that is equal to $\boldsymbol{\nu}^E$ on the interior of E and vanishes elsewhere.

The jump is defined as difference of the two one-sided limits at the common face of two neighbouring simplices. On a face E with adjacent simplices K^+, K^- and normal vector $\boldsymbol{\nu}^E$ pointing from K^+ to K^- the jump of $\mathbf{a} \in \mathcal{D}_k(\Omega)^d$ reads

$$[\mathbf{a}] := \mathbf{a}^+ - \mathbf{a}^-,$$

where $\mathbf{a}^+$ and $\mathbf{a}^-$ are the continuous extensions of $\mathbf{a}$ on $\overline{K^+}$ and $\overline{K^-}$, respectively. Hence, the jump in normal direction $[\mathbf{a}] \cdot \boldsymbol{\nu}^{\mathcal{F}_{\text{int}}}$ is invariant to flipping of the normals $\boldsymbol{\nu}^E$. The mean is defined by

$$\{\mathbf{a}\} := \frac{1}{2}(\mathbf{a}^+ + \mathbf{a}^-).$$

Also, note that by integrals of the kind

$$\int_{\partial K} \mathbf{f} \cdot \boldsymbol{\nu} \; d\sigma$$

for polynomials $\mathbf{f}$ on K, on $\partial\Omega$ we always allude the continuous extension of $\mathbf{f}|_K$ onto ∂K. Let

$$b_h^{\mathbf{m}}(\mathbf{u}, \mathbf{h}, \mathbf{m}) := \sum_{K \in \mathcal{T}(\Omega)} \int_K (\mathbf{u} \cdot \nabla)\mathbf{h} \cdot \mathbf{m} \; dx - \int_{\mathcal{F}_{\text{int}}} [\mathbf{h}] \cdot \{\mathbf{m}\}(\mathbf{u} \cdot \boldsymbol{\nu}^{\mathcal{F}_{\text{int}}}) \; d\sigma. \tag{3.5}$$

For an elaborate introduction to discrete finite element spaces we refer the reader to [13, 14]. To regularise f_1 and f_2, we proceed as follows. We take

$$f_1^{(s)}(c) := \frac{1}{g_s''(c)} = \max(s, c) \tag{3.6}$$

and

$$f_2^{(s)}(c) := \max(s, c)^{m-1} c. \tag{3.7}$$

Later on, we will also work with

$$\hat{f}_2^{(s)}(c) := \max(s, c)^m. \tag{3.8}$$

Note that f_2 only occurs in the numerator of (2.38d), hence no need for further regularisation. We also use discrete counterparts to the abbreviations

$$\mathbf{h} = \nabla R,$$
$$\hat{\mathbf{h}} = 2\alpha_1 + \beta \mathbf{h}_a,$$
$$\hat{\mathbf{b}} = \hat{\mathbf{h}} - 2\alpha_3 \mathbf{m},$$

see (2.12), (2.32). The precise definitions will be stated in (3.12g)-(3.14). Further intricacies arise due to the fact that on the other hand $\mathbf{m}$ has to be taken in $\mathcal{D}_1(\overline{\Omega})^d$ to allow for a discrete energy estimate (cf. choice of test functions in (3.21)). On the other hand, we have to give a definition for $\operatorname{curl} \mathbf{m}$ and for $\operatorname{div} \mathbf{m}$. Therefore, we introduce the space $H^1_{t0}(\Omega)^d$, see [10],

$$H^1_{t0}(\Omega)^d := \{\mathbf{N} \in H^1(\Omega)^d | \mathbf{N} \times \boldsymbol{\nu}|_{\partial\Omega} = 0\}.$$

We proceed by duality and define the discrete counterparts $\operatorname{curl}_h \mathbf{M}^k \in \mathcal{P}_1(\overline{\Omega})^d \cap H^1_{t0}(\Omega)^d$ and $\operatorname{div}_h \mathbf{M}^k \in \mathcal{P}_1(\overline{\Omega}) \cap H^1_0(\Omega)$ by the variational problems

$$\int_\Omega \mathcal{I}_{h,1}(\operatorname{curl}_h \mathbf{M}^k \cdot \mathbf{N}) \; dx = \int_\Omega \mathbf{M}^k \cdot \operatorname{curl} \mathbf{N} \; dx \quad \forall \mathbf{N} \in \mathcal{P}_1(\overline{\Omega}) \cap H^1_{t0}(\Omega)^d, \tag{3.9}$$

$$\int_\Omega \operatorname{div}_h \mathbf{M}^k S \; dx = \; - \int_\Omega \mathbf{M}^k \cdot \nabla S \; dx \quad \forall S \in \mathcal{P}_2(\overline{\Omega}) \cap H_0^1(\Omega). \tag{3.10}$$

By construction, $\operatorname{curl}_h \mathbf{M}^k \times \boldsymbol{\nu}|_{\partial\Omega} = 0$. Note that the choice of testfunctions also implies vanishing boundary values of the discrete divergence, consistent to our boundary condition $\operatorname{div} \mathbf{m}|_{\partial\Omega} = 0$. With those tools at hand, the discrete weak formulation is as follows. Starting with

$$\mathbf{U}^0 := \mathcal{I}_{h,2}^d(\mathbf{u}_0), \qquad c^0 := \mathcal{I}_{h,1}(c_0), \qquad \mathbf{M}^0 := \hat{\mathcal{I}}_{h,1}^d(\mathbf{m}_0), \tag{3.11}$$

for given continuous and square integrable initial data $\mathbf{u}_0$, c_0, $\mathbf{m}_0$, find for each timestep $k = 1, ..., n_T$ functions $(\mathbf{U}^k, P^k, c^k, \mathbf{V}^k_{\text{part}}, R^k, \mathbf{M}^k)$ in

$$\mathfrak{Y}_h := \mathcal{P}_2(\overline{\Omega})^d \times \mathcal{P}_1^{\text{mean}}(\overline{\Omega}) \times \mathcal{P}_1(\overline{\Omega}) \times \mathcal{P}_1(\overline{\Omega})^d \times \mathcal{P}_2^{\text{mean}}(\overline{\Omega}) \times \mathcal{D}_1(\overline{\Omega})^d$$

such that for all testfunctions $(\mathbf{V}, Q, \psi, \boldsymbol{\theta}, S, \mathbf{N}) \in \mathfrak{Y}_h$ the equations

$$\begin{aligned}
\rho_0 \int_\Omega \tfrac{(\mathbf{U}^k - \mathbf{U}^{k-1})}{\tau} \cdot \mathbf{V} \; dx - \int_\Omega P^k \operatorname{div} \mathbf{V} \; dx + 2\eta \int_\Omega \mathbf{D}\mathbf{U}^k : \mathbf{D}\mathbf{V} \; dx \\
+ \frac{\rho_0}{2} \int_\Omega (\mathbf{U}^{k-1} \cdot \nabla)\mathbf{U}^k \cdot \mathbf{V} \; dx - \frac{\rho_0}{2} \int_\Omega (\mathbf{U}^{k-1} \cdot \nabla)\mathbf{V} \cdot \mathbf{U}^k \; dx \\
= -D \int_\Omega c^{k-1} \nabla g_{s,h}'^k \cdot \mathbf{V} \; dx + \frac{\mu_0}{2} b_h^{\mathbf{m}}(\mathbf{V}, \underbrace{(2\alpha_1 \mathbf{H}^k + \beta(\mathbf{h}_a)_h^k - 2\alpha_3 \mathbf{M}^k)}_{\hat{\mathbf{B}}^k}, \mathbf{M}^k) \\
+ \frac{\mu_0}{4} \int_\Omega (\mathbf{M}^k \times \underbrace{(2\alpha_1 \mathbf{H}^k + \beta(\mathbf{h}_a)_h^k)}_{\hat{\mathbf{H}}^k}) \cdot \operatorname{curl} \mathbf{V} \; dx,
\end{aligned} \tag{3.12a}$$

$$\int_\Omega \operatorname{div} \mathbf{U}^k Q \; dx = 0, \tag{3.12b}$$

$$\int_\Omega \mathcal{I}_{h,1}\left(\tfrac{(c^k - c^{k-1})}{\tau} \psi\right) \; dx = \int_\Omega c^{k-1} \mathbf{U}^k \cdot \nabla \psi \; dx + \int_\Omega \hat{\mathcal{I}}_{h,1}(c^{k-1} \mathbf{V}^k_{\text{part}} \cdot \nabla \psi) \; dx, \tag{3.12c}$$

$$\begin{aligned}
\int_\Omega \mathcal{I}_{h,1}(\mathbf{V}^k_{\text{part}} \cdot \boldsymbol{\theta}) \; dx = -KD \int_\Omega \hat{\mathcal{I}}_{h,1}\left(\tfrac{f_{2,h}^{(s),k-1}}{f_{1,h}^{(s),k-1}} \nabla g_{s,h}'^k \cdot \boldsymbol{\theta}\right) \; dx \\
+ \frac{K\mu_0}{2} b_h^{\mathbf{m}}\left(\mathcal{I}_{h,1}^d\left(\frac{\hat{f}_{2,h}^{(s),k-1}}{(f_{1,h}^{(s),k-1})^2}\boldsymbol{\theta}\right), \underbrace{(2\alpha_1 \mathbf{H}^k + \beta(\mathbf{h}_a)_h^k - 2\alpha_3 \mathbf{M}^k)}_{\hat{\mathbf{B}}^k}, \mathbf{M}^k\right),
\end{aligned} \tag{3.12d}$$

$$\int_{\Omega'} \nabla R^k \cdot \nabla S \; dx = \int_{\Omega'} (\mathbf{h}_a)_h^k \cdot \nabla S \; dx - \int_\Omega \mathbf{M}^k \cdot \nabla S \; dx, \tag{3.12e}$$

$$\begin{aligned}
\int_\Omega \tfrac{(\mathbf{M}^k - \mathbf{M}^{k-1})}{\tau} \cdot \mathbf{N} \; dx - b_h^{\mathbf{m}}(\mathbf{U}^k, \mathbf{N}, \mathbf{M}^k) - b_h^{\mathbf{m}}\left(\mathbf{V}^k_{\text{part}}, \mathbf{N}, \mathbf{M}^k\right) \\
= \frac{1}{2} \int_\Omega \operatorname{curl} \mathbf{U}^k \times \mathbf{M}^k \cdot \mathbf{N} \; dx - \frac{1}{\tau_{\text{rel}}} \int_\Omega (\mathbf{M}^k - \chi_{r,h}^{k-1,k} \mathbf{H}^k) \cdot \mathbf{N} \; dx \\
- \sigma \int_\Omega \operatorname{curl} \operatorname{curl}_h \mathbf{M}^k \cdot \mathbf{N} \; dx + \sigma \int_\Omega \nabla \operatorname{div}_h \mathbf{M}^k \cdot \mathbf{N} \; dx
\end{aligned} \tag{3.12f}$$

hold[1]. The magnetic field strength $\mathbf{H}^k$ is defined by

$$\int_{\Omega'} \mathbf{H}^k \cdot \boldsymbol{\zeta}\ dx = \int_{\Omega'} \nabla R^k \cdot \boldsymbol{\zeta}\ dx \quad \forall \boldsymbol{\zeta} \in \mathcal{D}_1(\overline{\Omega'}), \tag{3.12g}$$

and the abbreviations $\hat{\mathbf{H}}^k, \hat{\mathbf{B}}^k$ are defined by

$$\hat{\mathbf{H}}^k = 2\alpha_1 \mathbf{H}^k + \beta(\mathbf{h}_a)_h^k, \tag{3.13}$$

$$\hat{\mathbf{B}}^k = \hat{\mathbf{H}}^k|_{\overline{\Omega}} - 2\alpha_3 \mathbf{M}^k. \tag{3.14}$$

Also note that the variational problem (3.12g) yields just the exact (weak) gradient of R^k on Ω as $\nabla \mathcal{P}_2(\overline{\Omega}) \subset \mathcal{D}_1(\overline{\Omega})$. Recall that in (3.12d),

$$\begin{aligned} \hat{\mathcal{I}}_{h,1}\left(\tfrac{f_{2,h}^{(s),k-1}}{f_{1,h}^{(s),k-1}} \nabla g_{s,h}'^k \cdot \boldsymbol{\theta}\right) &= \hat{\mathcal{I}}_{h,1}(\max(s, c^{k-1})^{m-2} c^{k-1} \nabla g_{s,h}'^k \cdot \boldsymbol{\theta}), \\ \mathcal{I}_{h,1}^d\left(\tfrac{\hat{f}_{2,h}^{(s),k-1}}{(f_{1,h}^{(s),k-1})^2} \boldsymbol{\theta}\right) &= \mathcal{I}_{h,1}^d(\max(s, c^{k-1})^{m-2} \boldsymbol{\theta}), \end{aligned} \tag{3.15}$$

which motivates the definition of

$$f_h^{(s),k-1} := \mathcal{I}_{h,1}(\max(s, c^{k-1})^{2-m}) \tag{3.16}$$

for later purposes in the discrete energy estimate. In addition, we define the discrete divergence of $\mathbf{H}^k$ as we use it later on,

$$\begin{aligned} \int_{\Omega} \operatorname{div}_h \mathbf{H}^k S\ dx &= -\int_{\Omega} \mathbf{H}^k \cdot \nabla S\ dx \quad \forall S \in \mathcal{P}_2(\overline{\Omega}) \cap H_0^1(\Omega), \\ \int_{\Omega' \setminus \Omega} \operatorname{div}_h \mathbf{H}^k S\ dx &= -\int_{\Omega' \setminus \Omega} \mathbf{H}^k \cdot \nabla S\ dx \quad \forall S \in \mathcal{P}_2(\Omega' \setminus \Omega) \cap H_0^1(\Omega' \setminus \Omega). \end{aligned} \tag{3.17}$$

We are using two definitions depending on the domain in order to underline that we cannot expect the divergence to exist globally in Ω' in the continuous setting. Furthermore, for given initial data $\mathbf{M}^0$ and external magnetic field $\mathbf{h}_a$ in timestep t^0 the magnetostatic equation (3.12e) is solvable. Hence, we define R^0 as solution of

$$\int_{\Omega'} \nabla R^0 \cdot \nabla S\ dx = \int_{\Omega'} (\mathbf{h}_a)_h^0 \cdot \nabla S\ dx - \int_{\Omega} \mathbf{M}^0 \cdot \nabla S\ dx \quad \forall S \in \mathcal{P}_2^{\text{mean}}(\overline{\Omega'}).$$

3.2. **Discrete energy estimate.** In this section, we show an energy estimate for the discrete scheme. In order to deal with the general case of arbitrary non-negative parameters $\alpha_0, \alpha_1, \alpha_2, \alpha_3$, we will use the regularized susceptibility $\chi_r(c, \mathbf{h})$ defined in (3.2).

[1]Note that the first two terms on the right hand side of (3.12a) contain discrete counterparts of $Dg'(c)\nabla c$ and $\mu_0(\nabla \mathbf{m})^T \mathbf{m}$ - two terms which are gradients and which therefore have been absorbed in ∇p in (2.38a).

Theorem 3.1. *Let* $(\mathbf{U}^k, P^k, c^k, \mathbf{V}^k_{\text{part}}, R^k, \mathbf{M}^k)_{k=0,\dots,n_T}$ *be a discrete solution to the scheme* (3.12)*. A positive constant* $C_0 := C_0(\alpha_1, \alpha_3, K_1, K_2, \tau_{\text{rel}}, \mathbf{h}_a, \sigma, \eta_r, \mu_0)$ *exists such that*

$$\begin{aligned}
&\frac{\rho_0}{2}\int_\Omega |\mathbf{U}^k|^2\,dx + D\int_\Omega g^k_{s,h}\,dx + \frac{\alpha_3\mu_0}{2}\int_\Omega |\mathbf{M}^k|^2\,dx + \frac{\mu_0\alpha_1}{2}\int_{\Omega'} |\nabla R^k|^2\,dx \\
&\quad + \frac{\rho_0}{2}\sum_{l=1}^k \int_\Omega |\mathbf{U}^l - \mathbf{U}^{l-1}|^2\,dx + \frac{\alpha_3\mu_0}{4}\sum_{l=1}^k\int_\Omega |\mathbf{M}^l - \mathbf{M}^{l-1}|^2\,dx \\
&\quad + \frac{\mu_0\alpha_1}{2}\sum_{l=1}^k\int_{\Omega'} |\nabla R^l - \nabla R^{l-1}|^2\,dx \\
&\quad + \tau\sum_{l=1}^k\int_\Omega 2\eta|\mathbf{D}\mathbf{U}^l|^2\,dx + \tau\sum_{l=1}^k\int_\Omega \hat{\mathcal{I}}_{h,1}\left(f^{l-1}_{s,h}\frac{|\mathbf{V}^l_{\text{part}}|^2}{K}\right)\,dx + \frac{\tau\mu_0\alpha_3}{2\tau_{\text{rel}}}\sum_{l=1}^k\int_\Omega |\mathbf{M}^l|^2\,dx \\
&\quad + \frac{\tau\sigma\mu_0\alpha_3}{2}\sum_{l=1}^k\int_\Omega |\operatorname{div}_h \mathbf{M}^l|^2\,dx + \frac{\tau\sigma\mu_0\alpha_1}{2}\sum_{l=1}^k\int_{\Omega'\setminus\partial\Omega} |\operatorname{div}_h \mathbf{H}^l|^2\,dx \\
&\quad + \frac{\tau\sigma\mu_0\alpha_3}{2}\sum_{l=1}^k\int_\Omega \mathcal{I}_{h,1}(|\operatorname{curl}_h \mathbf{M}^l|^2)\,dx + \frac{\tau\mu_0\alpha_1}{2\tau_{\text{rel}}}\sum_{l=1}^k\int_{\Omega'} |\nabla R^l|^2\,dx \\
&\quad + \frac{\tau\mu_0\alpha_1}{2\tau_{\text{rel}}}\sum_{l=1}^k\int_\Omega \chi^{l-1}_{r,h}|\mathbf{H}^l|^2\,dx \\
&\le \frac{\rho_0}{2}\int_\Omega |\mathbf{U}^0|^2\,dx + D\int_\Omega g^0_{s,h}\,dx + \frac{\alpha_3\mu_0}{2}\int_\Omega |\mathbf{M}^0|^2\,dx + \frac{\mu_0\alpha_1}{2}\int_{\Omega'} |\nabla R^0|^2\,dx + C_0.
\end{aligned} \tag{3.18}$$

Remark 3.2. *Estimate* (3.18) *may serve as the starting point to obtain convergence results for the numerical scheme* (3.12)*. Nevertheless, a number of intricacies still have to be addressed. Presumably, the most challenging one will be to obtain strong convergence of appropriate subsequences for the discrete magnetization* $\mathbf{M}$ *in appropriate Lebesgue spaces. This seems to be indispensable as the magnetization enters the particle velocity* $\mathbf{V}_{\text{part}}$ *in a nonlinear way (see* (2.38c)*,* (2.38d)*, and* (2.38f)*). In this respect, recall that the control of the* L^2*-norms of divergence and curl of a vector field in general does not imply the control of its gradient (cf., e.g., Proposition 2.7 in [7]). Therefore, convergence is beyond the scope of this paper.*

Proof: Test (3.12a) by $\tau\mathbf{U}^k$ and use (3.12b) to obtain

$$\begin{aligned}
&\frac{\rho_0}{2}\int_\Omega |\mathbf{U}^k|^2\,dx + \frac{\rho_0}{2}\int_\Omega |\mathbf{U}^k - \mathbf{U}^{k-1}|^2\,dx + \tau\int_\Omega 2\eta|\mathbf{D}\mathbf{U}^k|^2\,dx \\
&\quad = \frac{\rho_0}{2}\int_\Omega |\mathbf{U}^{k-1}|^2\,dx - \tau D\int_\Omega c^{k-1}\nabla g'^k_{s,h}\cdot\mathbf{U}^k\,dx \\
&\qquad + \frac{\tau\mu_0}{2}b^{\mathbf{m}}_h(\mathbf{U}^k, \hat{\mathbf{B}}^k, \mathbf{M}^k) + \frac{\tau\mu_0}{4}\int_\Omega (\mathbf{M}^k\times\hat{\mathbf{H}}^k)\cdot\operatorname{curl}\mathbf{U}^k\,dx.
\end{aligned} \tag{3.19}$$

We test (3.12d) by $\tau\mathcal{I}^d_{h,1}(f^{(s),k-1}_h\frac{\mathbf{V}^k_{\text{part}}}{K}) = \tau\mathcal{I}^d_{h,1}(\max(s,c^k)^{2-m}\frac{\mathbf{V}^k_{\text{part}}}{K})$ and (3.12c) by $\tau D g'^k_{s,h}$. First, we observe - remembering (3.15) and (3.16) - that

$$\int_\Omega \hat{\mathcal{I}}_{h,1}(\tfrac{f^{(s),k-1}_{2,h}}{f^{(s),k-1}_{1,h}}\nabla g'^k_{s,h}\cdot\mathcal{I}^d_{h,1}(f^{(s),k-1}_h\mathbf{V}^k_{\text{part}}))\,dx$$

$$= \int_\Omega \hat{\mathcal{I}}_{h,1}(\max(s,c^{k-1})^{m-2}c^{k-1}\nabla g'^k_{s,h}\cdot(\max(s,c^{k-1})^{2-m}\mathbf{V}^k_{\text{part}}))\ dx$$
$$= \int_\Omega \hat{\mathcal{I}}_{h,1}(c^{k-1}\nabla g'^k_{s,h}\cdot\mathbf{V}^k_{\text{part}})\ dx$$

and

$$\mathcal{I}^d_{h,1}\left(\frac{\hat{f}^{(s),k-1}_{2,h}}{(f^{(s),k-1}_{1,h})^2}\mathcal{I}^d_{h,1}(f^{(s),k-1}_h\mathbf{V}^k_{\text{part}})\right)$$
$$= \mathcal{I}^d_{h,1}\Big(\max(s,c^{k-1})^{m-2}(\max(s,c^{k-1})^{2-m}\mathbf{V}^k_{\text{part}})\Big)$$
$$= \mathcal{I}^d_{h,1}(\mathbf{V}^k_{\text{part}}) = \mathbf{V}^k_{\text{part}}.$$

Hence, we arrive at the equations

$$D\int_\Omega \mathcal{I}_{h,1}\left((c^k-c^{k-1})g'^k_{s,h}\right)\ dx = \tau D\int_\Omega c^{k-1}\mathbf{U}^k\cdot\nabla g'^k_{s,h}\ dx + \tau D\int_\Omega \hat{\mathcal{I}}_{h,1}(c^{k-1}\mathbf{V}^k_{\text{part}}\cdot\nabla g'^k_{s,h})\ dx$$

and

$$\tau\int_\Omega \mathcal{I}_{h,1}(f^{(s),k-1}_h\frac{|\mathbf{V}^k_{\text{part}}|^2}{K})\ dx = -\tau D\int_\Omega \hat{\mathcal{I}}_{h,1}(c^{k-1}\nabla g'^k_{s,h}\cdot\mathbf{V}^k_{\text{part}})\ dx + \frac{\tau\mu_0}{2}b^{\mathbf{m}}_h(\mathbf{V}^k_{\text{part}},\hat{\mathbf{B}}^k,\mathbf{M}^k).$$

Summing up, using the convexity of g_s and the choice $\mathcal{C}_h = \mathcal{P}_1(\overline{\Omega})$ we arrive at

$$\tau\int_\Omega \mathcal{I}_{h,1}\left(f^{(s),k-1}_h\frac{|\mathbf{V}^k_{\text{part}}|^2}{K}\right)\ dx + D\int_\Omega g^k_{s,h}\ dx \le D\int_\Omega g^{k-1}_{s,h}\ dx + \frac{\tau\mu_0}{2}b^{\mathbf{m}}_h(\mathbf{V}^k_{\text{part}},\hat{\mathbf{B}}^k,\mathbf{M}^k) + \tau D\int_\Omega c^{k-1}\mathbf{U}^k\cdot\nabla g'^k_{s,h}\ dx. \tag{3.20}$$

The magnetization (3.12f) will be tested by

$$-\frac{\tau\mu_0}{2}\hat{\mathbf{B}}^k = -\frac{\tau\mu_0}{2}(\hat{\mathbf{H}}^k - 2\alpha_3\mathbf{M}^k) = -\frac{\tau\mu_0}{2}(2\alpha_1\mathbf{H}^k|_{\overline{\Omega}} + \beta(\mathbf{h}_a)^k_h|_{\overline{\Omega}} - 2\alpha_3\mathbf{M}^k).$$

We get

$$\begin{aligned}
&-\frac{\mu_0}{2}\int_\Omega(\mathbf{M}^k-\mathbf{M}^{k-1})\cdot\hat{\mathbf{B}}^k\ dx + \frac{\tau\mu_0\alpha_3}{\tau_{\text{rel}}}\int_\Omega|\mathbf{M}^k|^2\ dx\\
&\quad-\frac{\tau\mu_0}{2\tau_{\text{rel}}}\int_\Omega\mathbf{M}^k\cdot\hat{\mathbf{H}}^k\ dx + \frac{\tau\mu_0}{2\tau_{\text{rel}}}\int_\Omega\chi^{k-1,k}_{r,h}\mathbf{H}^k\cdot\hat{\mathbf{H}}^k\ dx\\
&\qquad+\tau\sigma\mu_0\alpha_3\left(\int_\Omega\operatorname{curl}\operatorname{curl}_h\mathbf{M}^k\cdot\mathbf{M}^k\ dx - \int_\Omega\nabla\operatorname{div}_h\mathbf{M}^k\cdot\mathbf{M}^k\ dx\right)\\
&\qquad\quad-\frac{\tau\sigma\mu_0}{2}\left(\int_\Omega\operatorname{curl}\operatorname{curl}_h\mathbf{M}^k\cdot\hat{\mathbf{H}}^k\ dx - \int_\Omega\nabla\operatorname{div}_h\mathbf{M}^k\cdot\hat{\mathbf{H}}^k\ dx\right)\\
&= -\frac{\tau\mu_0}{2}b^{\mathbf{m}}_h(\mathbf{U}^k,\hat{\mathbf{B}}^k,\mathbf{M}^k) - \frac{\tau\mu_0}{2}b^{\mathbf{m}}_h\left(\mathbf{V}^k_{\text{part}},\hat{\mathbf{B}}^k,\mathbf{M}^k\right)\\
&\quad-\frac{\tau\mu_0}{4}\int_\Omega(\operatorname{curl}\mathbf{U}^k\times\mathbf{M}^k)\cdot\hat{\mathbf{H}}^k\ dx + \frac{\tau\mu_0\alpha_3}{\tau_{\text{rel}}}\int_\Omega\chi^{k-1,k}_{r,h}\mathbf{H}^k\cdot\mathbf{M}^k\ dx.
\end{aligned} \tag{3.21}$$

Using $2ab = -a^2 - b^2 + (a-b)^2$ the first term on the left hand side reads

$$\begin{aligned} &-\frac{\mu_0}{2}\int_\Omega (\mathbf{M}^k - \mathbf{M}^{k-1})\hat{\mathbf{B}}^k \, dx \\ &\quad = \frac{\alpha_3\mu_0}{2}\int_\Omega |\mathbf{M}^k|^2 \, dx - \frac{\alpha_3\mu_0}{2}\int_\Omega |\mathbf{M}^{k-1}|^2 \, dx + \frac{\alpha_3\mu_0}{2}\int_\Omega |\mathbf{M}^k - \mathbf{M}^{k-1}|^2 \, dx \\ &\qquad - \mu_0\alpha_1 \int_\Omega \mathbf{M}^k \cdot \mathbf{H}^k \, dx + \mu_0\alpha_1 \int_\Omega \mathbf{M}^{k-1} \cdot \mathbf{H}^k \, dx \\ &\qquad\quad - \frac{\mu_0\beta}{2}\int_\Omega (\mathbf{M}^k - \mathbf{M}^{k-1}) \cdot (\mathbf{h}_a)_h^k \, dx. \end{aligned} \tag{3.22}$$

We also test (3.12e) in timestep k and $k-1$ by $\mu_0\alpha_1 R^k$ and use (3.12g) to rewrite the second last and third last term on the right hand side of (3.22),

$$\begin{aligned} &-\mu_0\alpha_1 \int_\Omega \mathbf{M}^k \cdot \mathbf{H}^k \, dx + \mu_0\alpha_1 \int_\Omega \mathbf{M}^{k-1} \cdot \mathbf{H}^k \, dx \\ &\quad = -\mu_0\alpha_1 \int_\Omega \mathbf{M}^k \cdot \nabla R^k \, dx + \mu_0\alpha_1 \int_\Omega \mathbf{M}^{k-1} \cdot \nabla R^k \, dx \\ &\qquad = -\tau\mu_0\alpha_1 \int_{\Omega'} \left(\tfrac{(\mathbf{h}_a)_h^k - \mathbf{h}_a^{k-1}}{\tau} \right) \cdot \nabla R^k \, dx + \frac{\mu_0\alpha_1}{2}\int_{\Omega'} |\nabla R^k|^2 \, dx \\ &\qquad\quad - \frac{\mu_0\alpha_1}{2}\int_{\Omega'} |\nabla R^{k-1}|^2 \, dx + \frac{\mu_0\alpha_1}{2}\int_{\Omega'} |\nabla R^k - \nabla R^{k-1}|^2 \, dx. \end{aligned} \tag{3.23}$$

Analogously, in (3.21) we rewrite the third term of the left hand side

$$\begin{aligned} &-\frac{\tau\mu_0}{2\tau_{\mathrm{rel}}}\int_\Omega \mathbf{M}^k \cdot \hat{\mathbf{H}}^k \, dx \\ &= \frac{\tau\mu_0\alpha_1}{\tau_{\mathrm{rel}}}\int_{\Omega'} |\nabla R^k|^2 \, dx - \frac{\tau\mu_0\alpha_1}{\tau_{\mathrm{rel}}}\int_{\Omega'} (\mathbf{h}_a)_h^k \cdot \nabla R^k \, dx - \frac{\beta\tau\mu_0}{2\tau_{\mathrm{rel}}}\int_\Omega \mathbf{M}^k \cdot (\mathbf{h}_a)_h^k \, dx. \end{aligned} \tag{3.24}$$

The fourth term of the left hand side in (3.21) will be rewritten as follows,

$$\begin{aligned} &\frac{\tau\mu_0}{2\tau_{\mathrm{rel}}}\int_\Omega \chi_{r,h}^{k-1,k}\mathbf{H}^k \cdot \hat{\mathbf{H}}^k \, dx \\ &\quad = \frac{\tau\mu_0\alpha_1}{\tau_{\mathrm{rel}}}\int_\Omega \chi_{r,h}^{k-1,k}|\mathbf{H}^k|^2 \, dx + \frac{\beta\tau\mu_0}{2\tau_{\mathrm{rel}}}\int_\Omega \chi_{r,h}^{k-1,k}\mathbf{H}^k \cdot (\mathbf{h}_a)_h^k \, dx. \end{aligned} \tag{3.25}$$

Using the definitions (3.10) and (3.9), we get for the fifth and sixth term in the left hand side of (3.21)

$$\begin{aligned} &\tau\sigma\mu_0\alpha_3 \left(\int_\Omega \operatorname{curl}\operatorname{curl}_h \mathbf{M}^k \cdot \mathbf{M}^k \, dx - \int_\Omega \nabla \operatorname{div}_h \mathbf{M}^k \cdot \mathbf{M}^k \, dx \right) \\ &\quad = \tau\sigma\mu_0\alpha_3 \left(\int_\Omega \mathcal{I}_{h,1}(|\operatorname{curl}_h \mathbf{M}^k|^2) \, dx + \int_\Omega |\operatorname{div}_h \mathbf{M}^k|^2 \, dx \right). \end{aligned} \tag{3.26}$$

The seventh term on the left hand side of (3.21) will vanish by the following observations. Piecewise integration by parts, continuity of $R^k \in \mathcal{R}_h$ - implying continuity of tangential derivatives on $\partial K, K \in \mathcal{T}_h(\Omega)$ - and the boundary conditions enforced on $\operatorname{curl}_h \mathbf{M}^k$ by the

choice of testfunctions in (3.9) imply

$$
\begin{aligned}
&-\int_\Omega \operatorname{curl}\operatorname{curl}_h \mathbf{M}^k \cdot \nabla R^k \; dx \\
&\quad = -\sum_{K\in\mathcal{T}_h(\Omega)} \int_K \operatorname{curl}_h \mathbf{M}^k \cdot \underbrace{\operatorname{curl}\nabla R^k}_{=0} \; dx + \sum_{K\in\mathcal{T}_h(\Omega)} \int_{\partial K} \operatorname{curl}_h \mathbf{M}^k \times \boldsymbol{\nu} \cdot \nabla R^k \; d\sigma \\
&\quad = -\int_{\mathcal{F}_i} [\nabla R^k] \times \boldsymbol{\nu}^{\mathcal{F}_{\text{int}}} \cdot \operatorname{curl}_h \mathbf{M}^k \; d\sigma + \int_{\partial\Omega} \operatorname{curl}_h \mathbf{M}^k \times \boldsymbol{\nu} \cdot \nabla R^k \; d\sigma \\
&\quad = 0.
\end{aligned}
\tag{3.27}
$$

We continue discussing the eighth term on the left hand side of (3.21). We use (3.17) and test (3.12e) by $\operatorname{div}_h \mathbf{H}^k|_{\overline{\Omega}}$ and $\operatorname{div}_h \mathbf{H}^k|_{\Omega'\setminus\Omega}$ and find

$$
\begin{aligned}
\int_\Omega \nabla \operatorname{div}_h \mathbf{M}^k \cdot \nabla R^k \; dx &= -\int_\Omega \operatorname{div}_h \mathbf{M}^k \cdot \operatorname{div}_h \mathbf{H}^k \; dx \\
&= \int_\Omega \mathbf{M}^k \cdot \nabla \operatorname{div}_h \mathbf{H}^k \; dx \\
&= \int_{\Omega'\setminus\partial\Omega} \nabla \operatorname{div}_h \mathbf{H}^k \cdot (\mathbf{h}_a)_h^k \; dx - \int_{\Omega'\setminus\partial\Omega} \nabla \operatorname{div}_h \mathbf{H}^k \cdot \mathbf{H}^k \; dx \\
&= -\int_{\Omega'\setminus\partial\Omega} \operatorname{div}_h \mathbf{H}^k \cdot \operatorname{div}(\mathbf{h}_a)_h^k \; dx + \int_{\Omega'\setminus\partial\Omega} |\operatorname{div}_h \mathbf{H}^k|^2 \; dx.
\end{aligned}
\tag{3.28}
$$

We will rewrite the third term on the right hand side of (3.21) using

$$
(\operatorname{curl}\mathbf{U}^k \times \mathbf{M}^k) \cdot \hat{\mathbf{H}}^k = (\mathbf{M}^k \times \hat{\mathbf{H}}^k) \cdot \operatorname{curl}\mathbf{U}^k. \tag{3.29}
$$

Collecting the information in (3.21)-(3.29) and adding up the results (3.19) and (3.20) from before we obtain

$$
\begin{aligned}
&\frac{\rho_0}{2}\int_\Omega |\mathbf{U}^k|^2 \; dx - \frac{\rho_0}{2}\int_\Omega |\mathbf{U}^{k-1}|^2 \; dx + \frac{\rho_0}{2}\int_\Omega |\mathbf{U}^k - \mathbf{U}^{k-1}|^2 \; dx \\
&\quad + D\int_\Omega g_{s,h}^k \; dx - D\int_\Omega g_{s,h}^{k-1} \; dx \\
&\qquad + \frac{\alpha_3\mu_0}{2}\int_\Omega |\mathbf{M}^k|^2 \; dx - \frac{\alpha_3\mu_0}{2}\int_\Omega |\mathbf{M}^{k-1}|^2 \; dx + \frac{\alpha_3\mu_0}{2}\int_\Omega |\mathbf{M}^k - \mathbf{M}^{k-1}|^2 \; dx \\
&\qquad\quad + \frac{\mu_0\alpha_1}{2}\int_{\Omega'} |\nabla R^k|^2 \; dx - \frac{\mu_0\alpha_1}{2}\int_{\Omega'} |\nabla R^{k-1}|^2 \; dx + \frac{\mu_0\alpha_1}{2}\int_{\Omega'} |\nabla R^k - \nabla R^{k-1}|^2 \; dx \\
&\qquad\qquad + \tau\int_\Omega 2\eta|\mathbf{D}\mathbf{U}^k|^2 \; dx + \tau\int_\Omega \mathcal{I}_{h,1}\left(f_h^{(s),k-1}\frac{|\mathbf{V}_{\text{part}}^k|^2}{K}\right) \; dx \\
&\qquad\qquad\quad + \tau\sigma\mu_0\alpha_3\int_\Omega |\operatorname{div}_h \mathbf{M}^k|^2 \; dx + \tau\sigma\mu_0\alpha_1\int_{\Omega'\setminus\partial\Omega} |\operatorname{div}_h \mathbf{H}^k|^2 \; dx \\
&\qquad\qquad\qquad + \tau\sigma\mu_0\alpha_3\int_\Omega \mathcal{I}_{h,1}(|\operatorname{curl}_h \mathbf{M}^k|^2) \; dx + \frac{\tau\mu_0\alpha_3}{\tau_{\text{rel}}}\int_\Omega |\mathbf{M}^k|^2 \; dx \\
&\qquad\qquad\qquad\quad + \frac{\tau\mu_0\alpha_1}{\tau_{\text{rel}}}\int_{\Omega'} |\nabla R^k|^2 \; dx + \frac{\tau\mu_0\alpha_1}{\tau_{\text{rel}}}\int_\Omega \chi_{r,h}^{k-1,k}|\mathbf{H}^k|^2 \; dx
\end{aligned}
$$

$$
\begin{aligned}
&\leq \tau\mu_0\alpha_1 \int_{\Omega'} \left(\tfrac{(\mathbf{h}_a)_h^k - \mathbf{h}_a^{k-1}}{\tau}\right) \cdot \nabla R^k \, dx + \frac{\mu_0\beta}{2} \int_\Omega (\mathbf{M}^k - \mathbf{M}^{k-1}) \cdot (\mathbf{h}_a)_h^k \, dx \\
&\quad + \frac{\beta\tau\mu_0}{2\tau_{\mathrm{rel}}} \int_\Omega \mathbf{M}^k \cdot (\mathbf{h}_a)_h^k \, dx + \frac{\tau\mu_0\alpha_3}{\tau_{\mathrm{rel}}} \int_\Omega \chi_{r,h}^{k-1,k} \mathbf{H}^k \cdot \mathbf{M}^k \, dx \\
&\quad + \frac{\tau\mu_0\alpha_1}{\tau_{\mathrm{rel}}} \int_{\Omega'} (\mathbf{h}_a)_h^k \cdot \nabla R^k \, dx - \frac{\beta\tau\mu_0}{2\tau_{\mathrm{rel}}} \int_\Omega \chi_{r,h}^{k-1,k} \mathbf{H}^k \cdot (\mathbf{h}_a)_h^k \, dx \\
&\quad + \frac{\beta\tau\sigma\mu_0}{2} \int_\Omega \operatorname{div}_h \mathbf{M}^k \cdot \operatorname{div}(\mathbf{h}_a)_h^k \, dx + \alpha_1\tau\sigma\mu_0 \int_{\Omega'\setminus\partial\Omega} \operatorname{div}_h \mathbf{H}^k \cdot \operatorname{div}(\mathbf{h}_a)_h^k \, dx \\
&\quad + \frac{\beta\tau\sigma\mu_0}{2} \int_\Omega \operatorname{curl}_h \mathbf{M}^k \cdot \operatorname{curl}(\mathbf{h}_a)_h^k \, dx.
\end{aligned}
$$

Using $\mathbf{h}_a^k \in H^2(\overline{\Omega'})$, see (2.4), applying Young's inequality and absorption allows to bound all but the fourth and sixth term of the right hand side. The remaining terms are

$$
\left| \frac{\tau\mu_0\alpha_3}{\tau_{\mathrm{rel}}} \int_\Omega \chi_{r,h}^{k-1,k} \mathbf{H}^k \cdot \mathbf{M}^k \, dx \right| \leq \frac{\tau\mu_0\alpha_3}{2\tau_{\mathrm{rel}}} \int_\Omega |\mathbf{M}^k|^2 \, dx + \frac{\tau\mu_0\alpha_3}{2\tau_{\mathrm{rel}}} \int_\Omega |\chi_{r,h}^{k-1,k} \mathbf{H}^k|^2 \, dx
$$

and

$$
\left| \frac{\tau\mu_0\beta}{2\tau_{\mathrm{rel}}} \int_\Omega \chi_{r,h}^{k-1,k} \mathbf{H}^k \cdot (\mathbf{h}_a)_h^k \, dx \right| \leq \frac{\tau\mu_0|\beta|}{4\tau_{\mathrm{rel}}} \int_\Omega |(\mathbf{h}_a)_h^k|^2 \, dx + \frac{\tau\mu_0\beta}{4\tau_{\mathrm{rel}}} \int_\Omega |\chi_{r,h}^{k-1,k} \mathbf{H}^k|^2 \, dx.
$$

Note that the $|\mathbf{M}^k|^2$-term can be absorbed now and $\mathbf{h}_a$ is bounded. The norms $\|\cdot\|_{L^2(\Omega)}$ and $\left(\int_\Omega \hat{\mathcal{I}}_{h,1}(|\cdot|^2) \, dx\right)^{\frac{1}{2}}$ are equivalent independently from the mesh size. Therefore, we get

$$
\begin{aligned}
\int_\Omega |\chi_{r,h}^{k-1,k} \mathbf{H}^k|^2 \, dx &\leq C \int_\Omega \hat{\mathcal{I}}_{h,1} \left(\left| \hat{\mathcal{I}}_{h,1}(\chi_r(c^{k-1}, \mathbf{H}^k)) \mathbf{H}^k \right|^2 \right) \, dx \\
&= C \int_\Omega \hat{\mathcal{I}}_{h,1} \left(\left| \chi_r(c^{k-1}, \mathbf{H}^k) \mathbf{H}^k \right|^2 \right) \, dx \qquad (3.30) \\
&\leq \tilde{C} \int_\Omega |K_1 + K_2\sqrt{c^{k-1}}|^2 \, dx,
\end{aligned}
$$

where K_1, K_2 are the constants from (3.4) and $C, \tilde{C} > 0$ come from the norm equivalence. Note that $\|c^k\|_{L^1(\Omega)}$ is bounded by the entropy $\|g_{s,h}^k\|_{L^1(\Omega)}$, for instance

$$
\int_\Omega g_{s,h}^k \, dx \geq K_3 \int_\Omega |c^k| \, dx - K_4
$$

for some constants $K_3, K_4 > 0$ independent from the other parameters. Consequently, by absorption, summing over all timesteps and using Gronwall's lemma, the desired estimate follows. As in (3.30) the term $\|c^{k-1}\|_{L^1(\Omega)}$ appears at time t^{k-1} only, no restrictions on τ are necessary. □

Remark 3.3. *If one intends to use the linearized Langevin-formula, i.e. χ is given by*

$$
\chi_r(c, \mathbf{h}) = \chi_r(c) := \min(\max(0, \chi' c), r),
$$

(cf. (2.15), (2.16)*), then the following estimate leads to energy stability,*

$$
\frac{\tau\alpha_3\mu_0}{\tau_{\mathrm{rel}}} \int_\Omega \chi_{r,h}^{k-1,k} \mathbf{M}^k \cdot \mathbf{H}^k \, dx \leq \frac{1}{\delta} \frac{\tau\alpha_3\mu_0}{2\tau_{\mathrm{rel}} r} \int_\Omega \chi_{r,h}^{k-1,k} |\mathbf{M}^k|^2 \, dx + \delta \frac{\tau\alpha_3\mu_0 r}{2\tau_{\mathrm{rel}}} \int_\Omega \chi_{r,h}^{k-1,k} |\mathbf{H}^k|^2 \, dx
$$

$$\leq \frac{1}{\delta}\frac{\tau\alpha_3\mu_0}{2\tau_{\rm rel}}\int_\Omega |\mathbf{M}^k|^2\,dx + \delta\frac{\tau\alpha_3\mu_0 r}{2\tau_{\rm rel}}\int_\Omega \chi_{r,h}^{k-1,k}|\mathbf{H}^k|^2\,dx.$$

for any $\delta > 0$. For $\delta := \frac{\alpha_1}{\alpha_3 r}$ the second term on the right hand side can be absorbed and the estimate follows by Gronwall's lemma, which is applicable if

$$\tau < \delta = \frac{\alpha_1}{\alpha_3 r}.$$

Gronwall's lemma is not needed - hence restrictions on τ drop - if $\delta \geq 1$, which holds e.g. for $\alpha_3 \leq \frac{1}{r}$, $\alpha_1 \geq 1$.

4. Numerical results

In this section, we present first numerical simulations in 2D on the field-induced transport of magnetic nanoparticles in fluids. To reduce the numerical cost, we confine ourselves to the case $\Omega = \Omega'$. Some consequences on equations and boundary conditions are immediate. Adopting the notation of Dautray and Lions [10], we distinguish between the operators

$$\begin{aligned}\operatorname{curl} : C^1(\Omega)^2 &\to C(\Omega),\\ \operatorname{curl}\mathbf{v} &= \partial_{\mathbf{x}_1}\mathbf{v}_2 - \partial_{\mathbf{x}_2}\mathbf{v}_1\end{aligned}$$

and

$$\begin{aligned}\operatorname{Curl} : C^1(\Omega) &\to C(\Omega)^2,\\ \operatorname{Curl} v &= \begin{pmatrix}\partial_{\mathbf{x}_2} v\\ -\partial_{\mathbf{x}_1} v\end{pmatrix}.\end{aligned}$$

Similarly, for $\mathbf{a}, \mathbf{b} \in \mathbb{R}^2$ we define

$$\mathbf{a}\times\mathbf{b} := \mathbf{a}_1\mathbf{b}_2 - \mathbf{a}_2\mathbf{b}_1$$

and observe $\operatorname{curl}\mathbf{a} = \nabla\times\mathbf{a} = \partial_{\mathbf{x}_2}\mathbf{a}_1 - \partial_{\mathbf{x}_1}\mathbf{a}_2$. For a scalar function f, we introduce

$$f\times\mathbf{b} := f\begin{pmatrix}-\mathbf{b}_2\\ \mathbf{b}_1\end{pmatrix}.$$

Additionally, to simplify the implementation of the scheme, we use the linearized formula $\mathbf{m}_{\rm eq} = \chi_{\rm lin}(c)\mathbf{h}$ from (2.15), (2.16) and discretize

$$\chi_{\rm lin}(c) \approx \chi_{r,h}(c) := \mathcal{I}_{h,1}(\min(\max(0,\chi' c), r)),$$

where $\chi' > 0$ is the constant from (2.16) and $r > 0$ a cut-off parameter. With an additional explicit r-dependency of C_0 from Theorem 3.1 and, possibly, restrictions on τ the estimate from Theorem 3.1 remains valid, see Remark 3.3. This way, the evolution system under consideration is given by

$$\begin{aligned}&\rho_0\mathbf{u}_t + \rho_0(\mathbf{u}\cdot\nabla)\mathbf{u} + \nabla p - \operatorname{div}(2\eta\mathbf{D}\mathbf{u})\\ &\qquad = \mu_0(\mathbf{m}\cdot\nabla)(\alpha_1\mathbf{h} + \tfrac{\beta}{2}\mathbf{h}_a) + \frac{\mu_0}{2}\operatorname{Curl}(\mathbf{m}\times(\alpha_1\mathbf{h} + \tfrac{\beta}{2}\mathbf{h}_a)),\end{aligned} \tag{4.1a}$$

$$\operatorname{div}\mathbf{u} = 0, \tag{4.1b}$$

$$c_t + \mathbf{u}\cdot\nabla c + \operatorname{div}(c\mathbf{V}_{\rm part}) = 0, \tag{4.1c}$$

$$\mathbf{V}_{\rm part} = -KD\frac{f_2(c)}{c}\nabla g'(c) + K\mu_0\frac{f_2(c)}{c^2}(\nabla(\alpha_1\mathbf{h} + \tfrac{\beta}{2}\mathbf{h}_a - \alpha_3\mathbf{m}))^T\mathbf{m}, \tag{4.1d}$$

$$-\Delta R = -\operatorname{div}\mathbf{h} = \operatorname{div}\mathbf{m}, \tag{4.1e}$$

$$\mathbf{m}_t + \operatorname{div}(\mathbf{m} \otimes (\mathbf{u} + \mathbf{V}_{\text{part}})) - \sigma \nabla \operatorname{div} \mathbf{m} + \sigma \operatorname{Curl} \operatorname{curl} \mathbf{m} = \frac{1}{2} \operatorname{curl} \mathbf{u} \times \mathbf{m} - \frac{1}{\tau_{\text{rel}}} (\mathbf{m} - \chi_{\text{lin}}(c)\mathbf{h}), \tag{4.1f}$$

in $\Omega \times (0, T)$ subjected to the boundary conditions

$$\mathbf{u} = 0 \qquad \text{on } \partial\Omega \times [0, T], \tag{4.2a}$$

$$\mathbf{V}_{\text{part}} \cdot \boldsymbol{\nu} = 0 \qquad \text{on } \partial\Omega \times [0, T], \tag{4.2b}$$

$$\operatorname{div} \mathbf{m} = 0 \qquad \text{on } \partial\Omega \times [0, T], \tag{4.2c}$$

$$\operatorname{curl} \mathbf{m} \times \boldsymbol{\nu} = 0 \qquad \text{on } \partial\Omega \times [0, T], \tag{4.2d}$$

$$\nabla R \cdot \boldsymbol{\nu} = \mathbf{h} \cdot \boldsymbol{\nu} = (\mathbf{h}_a - \mathbf{m}) \cdot \boldsymbol{\nu} \qquad \text{on } \partial\Omega \times [0, T]. \tag{4.2e}$$

Observe that we use the identity $\Delta \mathbf{m} = \nabla \operatorname{div} \mathbf{m} - \operatorname{Curl} \operatorname{curl} \mathbf{m}$ which is consistent with the boundary conditions (2.21) and (2.22). This decomposition is widely used, see, e.g., [1, 27, 28].

Note that the boundary condition (4.2e) is a direct consequence of the weak formulation (2.27) for the choice $\Omega' = \Omega$. Concerning practical numerics, we have to take into account that particularly the evolution equation (4.1c) is expected to be convection dominant, because the diffusion of nanoparticles is rather weak, cf. the Einstein–Smoluchowski relation [16] for an estimate. Therefore, it seems reasonable to consider (4.1c) as a transport equation and to use upwinding techniques [22]. Hence, some parts of the system (4.1) will be solved using a finite-volume approach with the numerical flux controlled by min-mod-limiters. Our algorithm reads as follows.

Algorithm. The nonlinear system is solved using a fixed point iteration based on inner iterations. Starting from $\mathbf{M}^{k,0} := \mathbf{M}^{k-1}$, $\mathbf{U}^{k,0} := \mathbf{U}^{k-1}$, $c^{k,0} := c^{k-1}$ and $\mathbf{V}^{k,0}_{\text{part}} := \mathbf{V}^{k-1}_{\text{part}}$, the inner iteration scheme is as follows.

First, we compute new iterates for the discrete counterparts of equations (4.1e) and (4.1f) in spirit of (3.12e), (3.12f). For given $\mathbf{M}^{k,i-1}$, $\mathbf{U}^{k,i-1}$, $\mathbf{V}^{k,i-1}_{\text{part}}$, $i \geq 1$, we look for $\mathbf{M}^{k,i}, R^{k,i}$, such that for all $S \in \mathcal{P}_2^{\text{mean}}(\overline{\Omega'})$ and $\mathbf{N} \in \mathcal{D}_1(\overline{\Omega})^d$

$$\int_{\Omega'} \nabla R^{k,i} \cdot \nabla S \; dx = \int_{\Omega'} (\mathbf{h}_a)^k_h \cdot \nabla S \; dx - \int_{\Omega} \mathbf{M}^{k,i} \cdot \nabla S \; dx, \tag{4.3a}$$

$$\begin{aligned} &\int_{\Omega} \tfrac{(\mathbf{M}^{k,i} - \mathbf{M}^{k-1})}{\tau} \cdot \mathbf{N} \; dx - b^{\mathbf{m}}_h(\mathbf{U}^{k,i-1}, \mathbf{N}, \mathbf{M}^{k,i-1}) - b^{\mathbf{m}}_h\left(\mathbf{V}^{k,i-1}_{\text{part}}, \mathbf{N}, \mathbf{M}^{k,i-1}\right) \\ &\quad = \frac{1}{2} \int_{\Omega} \operatorname{curl} \mathbf{U}^{k,i-1} \times \mathbf{M}^{k,i-1} \cdot \mathbf{N} \; dx - \frac{1}{\tau_{\text{rel}}} \int_{\Omega} (\mathbf{M}^{k,i} - \chi^{k-1}_{r,h} \nabla R^{k,i}) \cdot \mathbf{N} \; dx \\ &\qquad - \sigma \int_{\Omega} \operatorname{Curl} \operatorname{curl}_h \mathbf{M}^{k,i-1} \cdot \mathbf{N} \; dx + \sigma \int_{\Omega} \nabla \operatorname{div}_h \mathbf{M}^{k,i-1} \cdot \mathbf{N} \; dx. \end{aligned} \tag{4.3b}$$

The scheme (4.3) is a linearized variant of the original problem. The inner solutions are obtained by solving the linear system of equations described by (4.3). Despite our frequent explicit choice of $\mathbf{M}^{k,i-1}$, we observe good convergence of the fixed point iteration.

Let us update the particle density. Before the discrete counterpart of equation (4.1c) can be solved, we have to determine the effective particle velocity $\mathbf{V}_{\text{part}}^{k,i-1}$ using the weak formulation. The convective velocity $\mathbf{V}_{\text{part}}^{k,i-1}$ (see (3.12d),(3.6)-(3.8)) will be computed for given $c^{k,i-1}$ by

$$\begin{aligned}\int_\Omega \mathcal{I}_{h,1}(\mathbf{V}_{\text{part}}^{k,i-1}\cdot\boldsymbol{\theta})\,dx &= -KD\int_\Omega \hat{\mathcal{I}}_{h,1}\Big(\tfrac{f_{2,h}^{(s),k-1}}{f_{1,h}^{(s),k-1}}\nabla g_{s,h}'^{k,i-1}\cdot\boldsymbol{\theta}\Big)\,dx \\ &\quad + \frac{K\mu_0}{2}b_h^{\mathbf{m}}\left(\mathcal{I}_{h,1}^d\left(\frac{\hat{f}_{2,h}^{(s),k-1}}{(f_{1,h}^{(s),k-1})^2}\boldsymbol{\theta}\right),\hat{\mathbf{B}}^{k,i},\mathbf{M}^{k,i}\right) \qquad \forall\boldsymbol{\theta}\in\mathcal{P}_1(\overline{\Omega})^d, \end{aligned} \tag{4.4a}$$

where the quantities $\mathbf{M}^{k,i}$ and $\hat{\mathbf{B}}^{k,i}=\hat{\mathbf{B}}^{k,i}(\mathbf{M}^{k,i},R^{k,i},(\mathbf{h}_a)_h^k)$, analogously defined to (3.14), are already given by the solutions of the sub-problem (4.3). To determine a new iterate for c, we consider the dual mesh associated to the triangulation $\mathcal{T}_h$. Given a nodal point $\mathbf{x}_j\in\overline{\Omega}$, we consider the dual cell

$$V_j := \{\mathbf{x}\in\Omega \,|\, |\mathbf{x}_j-\mathbf{x}|<|\mathbf{x}_l-\mathbf{x}|\ \forall l=1,...,\dim\mathcal{P}_1(\overline{\Omega}), l\neq j\} \quad \forall j=1,...,\dim\mathcal{P}_1(\overline{\Omega}).$$

For a given function $c\in\mathcal{P}_1(\overline{\Omega})$, a corresponding cell-wise constant finite-volume function c^{FV} is readily defined by

$$c^{\text{FV}}|_{V_j} := c(\mathbf{x}_j) \text{ for each } j\in\{1,...,\dim\mathcal{P}_1(\overline{\Omega})\}.$$

We obtain an intermediate solution $c^{k-\frac{1}{2},i}$ by the following finite volume discretization. Find nodal values $c^{k-\frac{1}{2},i}(\mathbf{x}_l)$, $l=1,...,\dim\mathcal{P}_1(\overline{\Omega})$, such that for all $j=1,...,\dim\mathcal{P}_1(\overline{\Omega})$ (correlated to testfunctions $\psi=\mathbb{1}_{V_j}$)

$$\frac{|V_j|}{\tau}(c^{k-\frac{1}{2},i}(\mathbf{x}_j)-c^{k-1}(\mathbf{x}_j)) + \sum_{n\in\mathcal{N}_j} F_{jn}(\mathbf{U}^{k,i-1}+\mathbf{V}_{\text{part}}^{k,i-1},c^{k-1}(\mathbf{x}_j),c^{k-1}(\mathbf{x}_n)) = 0, \tag{4.4b}$$

where $\mathcal{N}_j$ is the index set of those neighbouring dual cells, which share a common face with the cell V_j. For the numerical flux $F_{jn}(\mathbf{U}^{k,i-1}+\mathbf{V}_{\text{part}}^{k,i-1},\cdot,\cdot)$ we choose the Engquist-Osher-flux with min-mod-limiter [22]. We then compute a finite element function $c^{k,i}$ by piecewise linear nodal interpolation of the values $c^{k-\frac{1}{2},i}(\mathbf{x}_j)$, $j=1,...,\dim\mathcal{P}_1(\overline{\Omega})$. Afterwards, we can update $\mathbf{V}_{\text{part}}^{k,i-1}$ to $\mathbf{V}_{\text{part}}^{k,i}$ by replacing $g_{s,h}'^{k,i-1}$ by $g_{s,h}'^{k,i}$ in (4.4b). Note that $c^{k,i}$, $\mathbf{V}_{\text{part}}^{k,i}$ (and $\mathbf{V}_{\text{part}}^{k,i-1}$) are computed explicitly.

At last, using the intermediate solutions that have been computed so far, the Navier-Stokes equations can be solved as follows. Let $\hat{\mathbf{H}}^{k,i}$, $\hat{\mathbf{B}}^{k,i}$ be defined as in (3.13),(3.14). Find $\mathbf{U}^{k,i}$, $P^{k,i}$, such that for all $\mathbf{V}\in\mathcal{P}_2(\overline{\Omega})^d$, $Q\in\mathcal{P}_1^{\text{mean}}(\overline{\Omega})$

$$\begin{aligned}\rho_0\int_\Omega \tfrac{(\mathbf{U}^{k,i}-\mathbf{U}^{k-1})}{\tau}\cdot\mathbf{V}\,dx - \int_\Omega P^{k,i}\operatorname{div}\mathbf{V}\,dx + 2\eta\int_\Omega \mathbf{D}\mathbf{U}^k:\mathbf{D}\mathbf{V}\,dx \\ + \frac{\rho_0}{2}\int_\Omega(\mathbf{U}^{k-1}\cdot\nabla)\mathbf{U}^k\cdot\mathbf{V}\,dx - \frac{\rho_0}{2}\int_\Omega(\mathbf{U}^{k-1}\cdot\nabla)\mathbf{V}\cdot\mathbf{U}^k\,dx \\ = -D\int_\Omega c^{k-1}\nabla g_{s,h}'^{k,i}\cdot\mathbf{V}\,dx + \frac{\mu_0}{2}b_h^{\mathbf{m}}(\mathbf{V},\hat{\mathbf{B}}^{k,i},\mathbf{M}^{k,i}) \\ + \frac{\mu_0}{4}\int_\Omega(\mathbf{M}^{k,i}\times\hat{\mathbf{H}}^{k,i})\cdot\operatorname{curl}\mathbf{V}\,dx,\end{aligned} \tag{4.5}$$

$$\int_\Omega \operatorname{div} \mathbf{U}^{k,i} Q \, dx = 0. \tag{4.6}$$

We can, finally, obtain $\mathbf{U}^{k,i}, P^{k,i}$ by solving a saddle-point problem of the type

$$\begin{pmatrix} \mathbf{A} & \mathbf{B}^T \\ \mathbf{B} & \mathbf{0} \end{pmatrix} \begin{pmatrix} \overline{\mathbf{U}^{k,i}} \\ \overline{P^{k,i}} \end{pmatrix} = \begin{pmatrix} \mathbf{f} \\ \mathbf{0} \end{pmatrix},$$

where the right hand side $\mathbf{f}$ depends on given data from the previous timestep or inner iterations of the sub-problems (4.3),(4.4) and the vectors $\overline{\mathbf{U}^{k,i}}, \overline{P^{k,i}}$ contain the degrees of freedom of the unknowns $\mathbf{U}^{k,i}, P^{k,i}$.

Finally, in the computations to be presented below, we use the stopping criteria

$$|\overline{\mathbf{U}^{k,i}} - \overline{\mathbf{U}^{k,i-1}}|^2 \le 10^{-12}, \qquad |\overline{P^{k,i}} - \overline{P^{k,i-1}}|^2 \le 10^{-10},$$
$$|\overline{\mathbf{M}^{k,i}} - \overline{\mathbf{M}^{k,i-1}}|^2 \le 10^{-12}, \quad |\overline{\nabla R^{k,i}} - \overline{\nabla R^{k,i-1}}|^2 \le 10^{-12}, \qquad |\overline{R^{k,i}} - \overline{R^{k,i-1}}|^2 \le 10^{-16},$$
$$|\overline{c^{k,i}} - \overline{c^{k,i-1}_{\text{part}}}|^2 \le 10^{-12}, \quad |\overline{\mathbf{V}^{k,i}_{\text{part}}} - \overline{\mathbf{V}^{k,i-1}_{\text{part}}}|^2 \le 10^{-10}.$$

for the inner iterations, where the bars denote the degrees of freedom of the underlying finite-element functions. Note that we consider $\mathbf{H}^{k,i} = \nabla R^{k,i}$ too, as it appears in our system of equations quite often.

Adaptivity in space and time. First, we discuss our choice of time increments. For upwinding schemes, the time increment τ should be chosen adaptively depending on $\mathbf{u}$ and $\mathbf{V}_{\text{part}}$. In particular, $\mathbf{V}_{\text{part}}$ is not constant in space or time. Moreover, it contains implicit terms. Therefore we pursue a heuristic approach. Our concept for adaptivity with respect to time is based on two pillars,

(P1) the CFL-condition $\tau \le C \frac{h}{|\mathbf{v}|}$ (cf. [22]) where $\mathbf{v}$ is a typical transport velocity to be specified later, h is the minimum mesh size and C is the CFL-coefficient, often taken $C = 1$ for scalar conservation laws,

(P2) the approach to choose the time increment such small that

$$c^k = c^{k-1} - \tau \operatorname{div}(c^{k-1}(\mathbf{V}^k_{\text{part}})_{\text{mag}}) \overset{!}{\ge} 0, \tag{4.7}$$

where $(\mathbf{V}^k_{\text{part}})_{\text{mag}}$ contains only the contributions to $\mathbf{V}^k_{\text{part}}$ coming from magnetic quantities. This approach will be combined with a minimum time increment $\tau_{\min}$ to be specified later on.

Note that we may use only data arising in the timesteps $k-1$ and $k-2$ to determine the increment for the transition $k-1 \to k$. In the beginning not all data are available yet, e.g. for $k = 0$ data in timestep $k-1 = -1$ do not exist. Unavailable data will then be set equal to initial data. Hence, our concept reads as follows, where we use parameters $C_1 := \frac{0.1}{\sqrt{2}}, C_2 := 0.1$, $(\varepsilon_{\text{abs},i})_{i=1,2} := (10^{-5}, 10^{-9})$, $\varepsilon_{\text{rel}} := 10^{-5}$ and $\tau_{\text{init}} = 10^{-3}$, $\tau_{\min} = 10^{-7}$.
ad P1:

1) For all nodes i, compute

$$\mathbf{v}(i) := \begin{cases} \|\mathbf{U}^{k-1}(\mathbf{x}_i) + (\mathbf{V}^{k-1}_{\text{part}})_{\text{mag}}(\mathbf{x}_i)\|_2 & \text{if } c^{k-1}(\mathbf{x}_i) > \max_i |c^{k-1}(\mathbf{x}_i)|\varepsilon_{\text{rel}}, \\ 0 & \text{else.} \end{cases}$$

2) Set $\tau_0 := \min(\tau_{\text{init}}, \frac{h}{\max_i \mathbf{v}(i)} C_1)$.

ad P2:

1) Compute $(\mathbf{V}^{k-1}_{\text{part}})_{\text{mag}}$ in spirit of (4.1d) without the diffusive term and compute an approximation of $\operatorname{div}(c^{k-1}(\mathbf{V}^{k}_{\text{part}})_{\text{mag}})$, cf. (4.7), called $\text{speed}^{k-1}_{\text{mag}} \in \mathcal{P}_1(\overline{\Omega})$, by the variational formulation
$$-\int_\Omega \mathcal{I}_{h,1}(\text{speed}^{k-1}_{\text{mag}}\psi)\ dx = \int_\Omega c^{k-2}(\mathbf{V}^{k-1}_{\text{part}})_{\text{mag}} \cdot \nabla\psi\ dx \quad \forall \psi \in \mathcal{P}_1(\overline{\Omega}).$$
2) For all nodes i, take
$$\tau(i) := \begin{cases} \frac{c^{k-1}(\mathbf{x}_i)}{\max(\varepsilon_{\text{abs},1}, \text{speed}^{k-1}_{\text{mag}}(\mathbf{x}_i))} & \text{if } c^{k-1}(\mathbf{x}_i) > \varepsilon_{\text{abs},2} \text{ and } \text{speed}^{k-1}_{\text{mag}}(\mathbf{x}_i) \geq 0, \\ \infty & \text{else.} \end{cases}$$
3) Set $\tau_1 := \min(\tau_{\text{init}}, C_2 \min_i \tau(i))$.
4) Approximate the effective transport velocity of the future timestep k using
$$\text{speed}^{k}_{\text{mag}} := 2\text{speed}^{k-1}_{\text{mag}} - \text{speed}^{k-2}_{\text{mag}},$$
which assumes $\text{speed}^{k-1}_{\text{mag}}$ to be at first order the arithmetic mean of $\text{speed}^{k-2}_{\text{mag}}$ and $\text{speed}^{k}_{\text{mag}}$.
5) Proceed as in 2.2), but replacing $\text{speed}^{k-1}_{\text{mag}}$ by the approximation $\text{speed}^{k}_{\text{mag}}$ in order to get the nodal time increments $\tilde{\tau}(i)$.
6) Set $\tau_2 := \min(\tau_{\text{init}}, C_2 \min_i \tilde{\tau}(i))$.

Then, choose the time increment as $\tau := \max(\tau_{\min}, \frac{1}{3}(\tau_0 + \tau_1 + \tau_2))$.

Our concept of adaptivity with respect to space is partially motivated by the phenomena which we expect to observe. Large values and large changes of magnetization field and stray field should not occur far away from the nanoparticles' support. Therefore we refine certain neighbourhoods of the current support of c^{k-1}. More precisely, let $d_{i,j}$, $i, j = 1, ..., \dim \mathcal{P}_1(\overline{\Omega})$ formally be the pseudo-distances
$$d_{i,j} := \begin{cases} \|\mathbf{x}_i - \mathbf{x}_j\|_\infty & \text{if } c^{k-1}(\mathbf{x}_j) > \delta_{\text{rel}} \max_l |c^{k-1}(\mathbf{x}_l)| \text{ and } c^{k-1}(\mathbf{x}_j) > \delta_{\text{abs}}, \\ \infty & \text{else} \end{cases}$$
between nodes i and j. Note that $d_{i,j}$ is infinite if node j is not contained in the essential support of the particle density function - defined by absolute and relative thresholds $\delta_{\text{abs}} = 5 \cdot 10^{-5}$ and $\delta_{\text{rel}} = 1 \cdot 10^{-3}$. Define
$$\hat{d}_i := \min_j d_{i,j}.$$
Then a node i gets marked for refinement if $\hat{d}_i < C_d$, where $C_d = \frac{4}{\sqrt{2}}h$ is the distance of the neighbourhood from the essential support of the particles.

Magnetic field. For our applied magnetic field we use a dipole potential
$$\phi_s(\mathbf{x}) := C_s \frac{\mathbf{d} \cdot (\mathbf{x}_s - \mathbf{x})}{\|\mathbf{x}_s - \mathbf{x}\|^2},$$
with director $\mathbf{d}$ and location at $\mathbf{x}_s \in \mathbb{R}^2 \setminus \Omega'$. The intensity of the dipole is scaled by $C_s \geq 0$. As ϕ_s is harmonic and $\mathbf{x}_s \notin \Omega'$, the choice
$$\mathbf{h}_a(\mathbf{x}, t) = I(t)\nabla\phi_s(\mathbf{x})$$

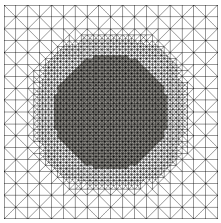

FIGURE 4.1. Triangular mesh illustrated by black lines. The gray colored region indicates $c \geq 0.001 \max_\Omega c$, where the maximum is 1.

with bounded intensity parameter $I(\cdot)$ is consistent with the requirements in Section 2. More precisely, we take

$$I(t) = \min(\max(0, t/0.01), 1).$$

More data and regularisation parameters. In the simulations below, we take the parameters

$$(\alpha_0, \alpha_1, \alpha_2, \alpha_3) = (1, 1, 1, 0.01).$$

Hence, the magnetic energy is given by $\mathcal{E}_{\text{mag}} = \frac{\mu_0}{2} \int_{\Omega'} |\mathbf{h}|^2 \, dx + 0.01 \frac{\mu_0}{2} \int_\Omega |\mathbf{m}|^2 \, dx$. For the Kelvin force, we have $\mu_0(\mathbf{m} \cdot \nabla)\mathbf{h} - 0.001\mu_0(\nabla \mathbf{m})^T \mathbf{m}$ with the second term being a gradient - hence it can be absorbed in the pressure gradient. For the diffusivity f_2 in the particle evolution equation, we take

$$f_2(c) = c$$

implying

$$f_{2,h}^{(s),k-1} = c, \qquad \hat{f}_{2,h}^{(s),k-1} = \max(s, c),$$

with the cut-off parmeter $s = 10^{-3}$ ($m = 1$ in (3.7), (3.8)). We use the linear susceptibility from (2.16), however regularized by a threshold parameter $r = 10^7$, giving altogether

$$\chi_r(c) = \min(\max(0, \chi' c), r).$$

As computational domain, we take $\Omega = \Omega' = (0, 1)^2$. Initial data for the particle density are given by

$$c^0(\mathbf{x}) := \begin{cases} \frac{1}{2}(\cos(\frac{|\mathbf{x}-\mathbf{y}|^2}{r^2}\pi) + 1) & \text{if } \frac{|\mathbf{x}-\mathbf{y}|^2}{r^2} \leq 1 \\ 0 & \text{else,} \end{cases}$$

with $\mathbf{y} := (0.5, 0.5)$, modeling a particle accumulation of circular shape with zero "contact-angle" at the boundary of its support. Initial data for velocity field and magnetization are taken zero.

Numerical results. We present snapshots of two numerical experiments which differ from each other by the location and maximum intensity of the magnetic dipole which is used to drive the evolution. In our first simulation, it is placed at $\mathbf{x}_s = (3, 0.5)$ with the maximum intensity given by $C_s = 100$. Table 1 gives an overview about further model parameters. Taking $\chi' = 1$, we find the susceptibility to be in the range of commercial ferrofluids. Figure 4.2 illustrates the initial configuration - observe the slightly curved streamlines of the external field $\mathbf{h}_a$. This is in contrast to the snapshots in Figure 4.3, which show the transport of the magnetic nanoparticles towards the right boundary of

ρ_0	η	χ'	μ_0	σ	τ_{rel}	K	D
1000	1	1	$4\pi \cdot 10^{-7}$	0.01	10^{-5}	500	10^{-6}

τ	h
$\in (10^{-7}, 10^{-3}]$	$\in [0.0125, 0.05]$

TABLE 1. Choice of parameters used in the computations.

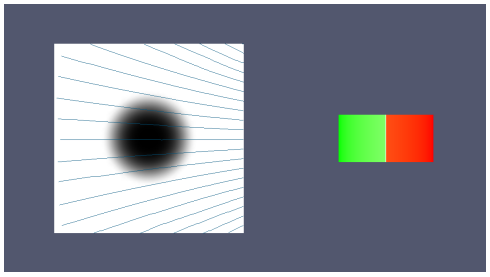

FIGURE 4.2. Artificial illustration of initial data, simulation domain and dipole position. Black color means high concentration, white color means $c = 0$. Blue lines indicate (only in this figure) the maximum applied external field $\mathbf{h}_a$, i.e. $\mathbf{h}_a$ at the time $t = 0.01$. Position of the dipole (green/red bar) is not up to scale.

Ω. In Figure 4.3, the blue streamlines show the magnetic field $\mathbf{h}$. It is clearly visible how $\mathbf{h}_a$ and $\mathbf{h}$ differ in those regions where the particle density is high and therefore large values of the demagnetizing field $\mathbf{h}_d$ are to be expected. In the course of time, this disturbance vanishes as the particles accumulate at the right boundary of Ω. Level lines of the particles density c are shown as gray contour lines. The snapshot Figure 4.3o indicates the tendency of level lines of c to be perpendicular to the streamlines of $\mathbf{h}$. However, in a finite distance to the upper and lower boundaries of Ω, this orthogonality still at time $t = 16$ is not perfect - presumably the result of the peak formation at the upper and lower boundaries visible at intermediate times $t \in \{1.6, 1.92, 2.56\}$. Figure 4.4 informs about the time evolution of the stray field $\mathbf{h}_d$ which is plotted using arrows. For the interpretation of the diagrams, it is important to note that the arrows are normalized. Hence, it is their color which provides information about their magnitude (the darker - the smaller). The magnetization field $\mathbf{m}$ is visualized by red-green bars - scaled according to their magnitude.

Snapshots of our second numerical experiment are depicted in Figure 4.5. The scope has been to investigate how the evolution is changed in a magnetic field whose expected magnetic body force is of the same order but with streamlines more curved. For this, we place the dipole more closely towards the domain, taking $\mathbf{x}_s = (1.75, 0.5)$, while reducing at the same time its maximum intensity to $C_s = 5$. We observe that the closer $\mathbf{x}$ approaches $\mathbf{x}_0 = 1$, the magnetic stream lines are perpendicular to the level lines of c. Looking at the green/red bars which visualize the magnetization, in particular in Figure 4.5f, we observe that the size of magnetization is the higher, the larger the particle density is. This is a nice indication that indeed the magnetization field is strongly coupled to the particles and transported with the particle flow.

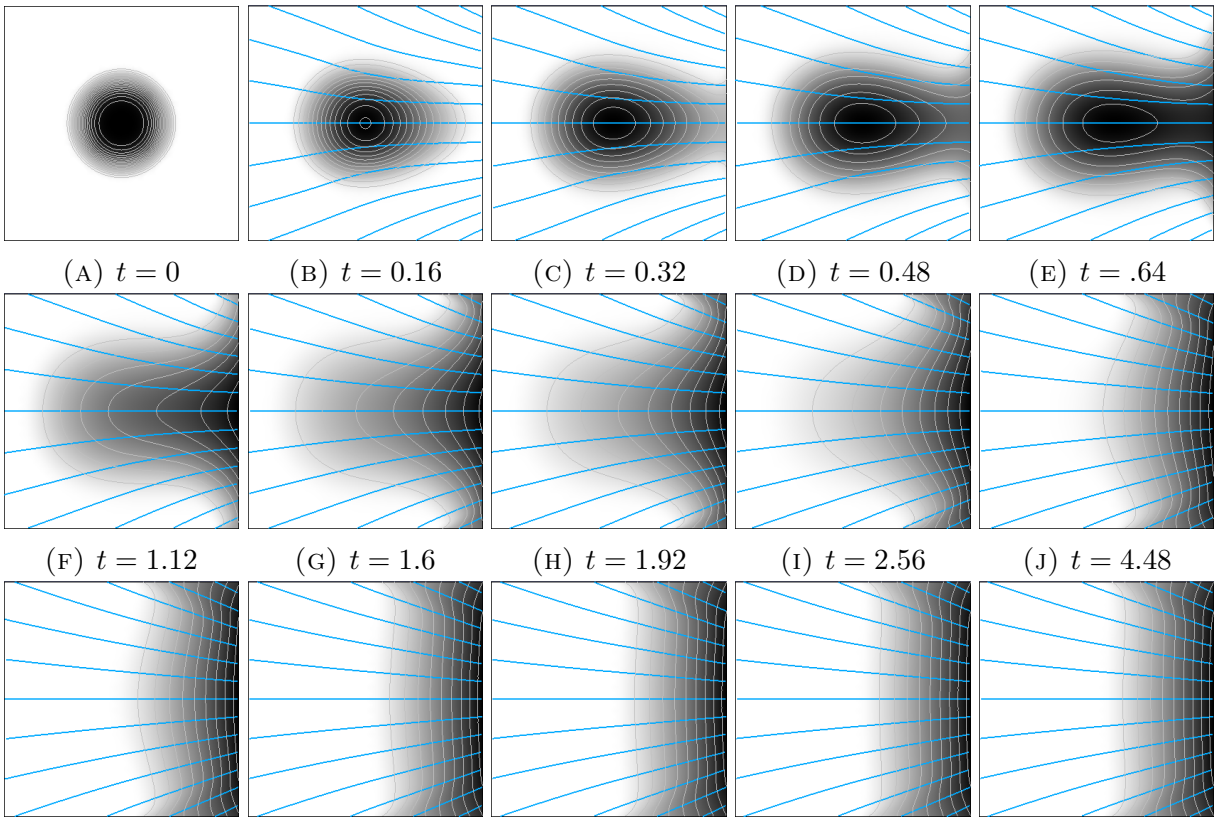

(A) $t = 0$ (B) $t = 0.16$ (C) $t = 0.32$ (D) $t = 0.48$ (E) $t = .64$

(F) $t = 1.12$ (G) $t = 1.6$ (H) $t = 1.92$ (I) $t = 2.56$ (J) $t = 4.48$

(K) $t = 5.6$ (L) $t = 7.2$ (M) $t = 8$ (N) $t = 12.8$ (O) $t = 16$

FIGURE 4.3. Particle density visualized by black color levels, where darker indicates higher density. Blue lines resemble the magnetic field lines of the total field $\mathbf{h}$, gray lines indicate contour lines of c. Dipole is located at $\mathbf{x}_s = (3, 0.5)$ with intensity $C_s = 100$.

Acknowledgment. The authors gratefully acknowledge support by Friedrich-Alexander-Universität Erlangen-Nürnberg and STAEDTLER Foundation through the project "Molecular Communication Systems" in the framework of the Emerging Fields Initiative as well as by German Science Foundation (DFG) through the Research Training Group (Graduiertenkolleg) 2339 “Interfaces, Complex Structures, and Singular Limits in Continuum Mechanics”.

REFERENCES

1. Y. Amirat and K. Hamdache, *Global weak solutions to a ferrofluid flow model*, Mathematical Methods in the Applied Sciences **31** (2008), no. 2, 123–151.
2. _____, *Weak solutions to the equations of motion for compressible magnetic fluids*, Journal de Mathématiques Pures et Appliquées **91** (2009), no. 5, 433–467.
3. _____, *Heat transfer in incompressible magnetic fluid*, Journal of Mathematical Fluid Mechanics **14** (2012), no. 2, 217–247.
4. _____, *On a heated incompressible magnetic fluid model*, Communications on Pure and Applied Analysis **11** (2012), 675–696.

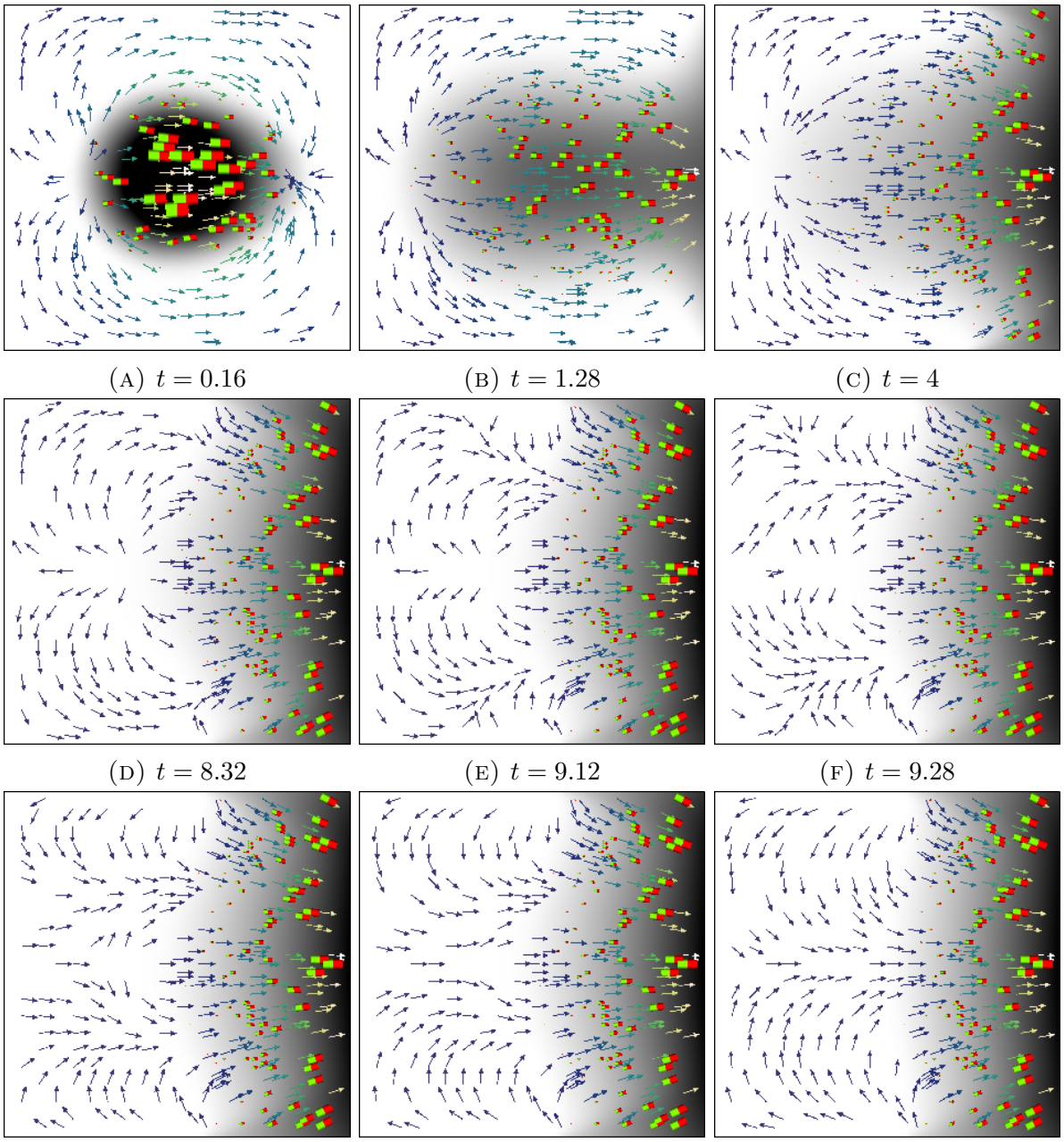

(A) $t = 0.16$ (B) $t = 1.28$ (C) $t = 4$

(D) $t = 8.32$ (E) $t = 9.12$ (F) $t = 9.28$

(G) $t = 9.44$ (H) $t = 9.6$ (I) $t = 11.68$

FIGURE 4.4. Particle density visualized by black color levels, where darker indicates higher density. Normalized arrows indicating stray field $\mathbf{h}_d$, brighter color means stronger magnitude. Red/green cylinders visualize magnetization $\mathbf{m}$. Dipole at $\mathbf{x}_s = (3, 0.5)$ with intensity $C_s = 100$.

5. _____, *Strong solutions to the equations of flow and heat transfer in magnetic fluids with internal rotations*, Discrete and Continuous Dynamical Systems - Series A (DCDS-A) **33** (2013), no. 8, 3289–3320.

6. _____, *Strong solutions to the equations of electrically conductive magnetic fluids*, Journal of Mathematical Analysis and Applications **421** (2015), no. 1, 75–104.

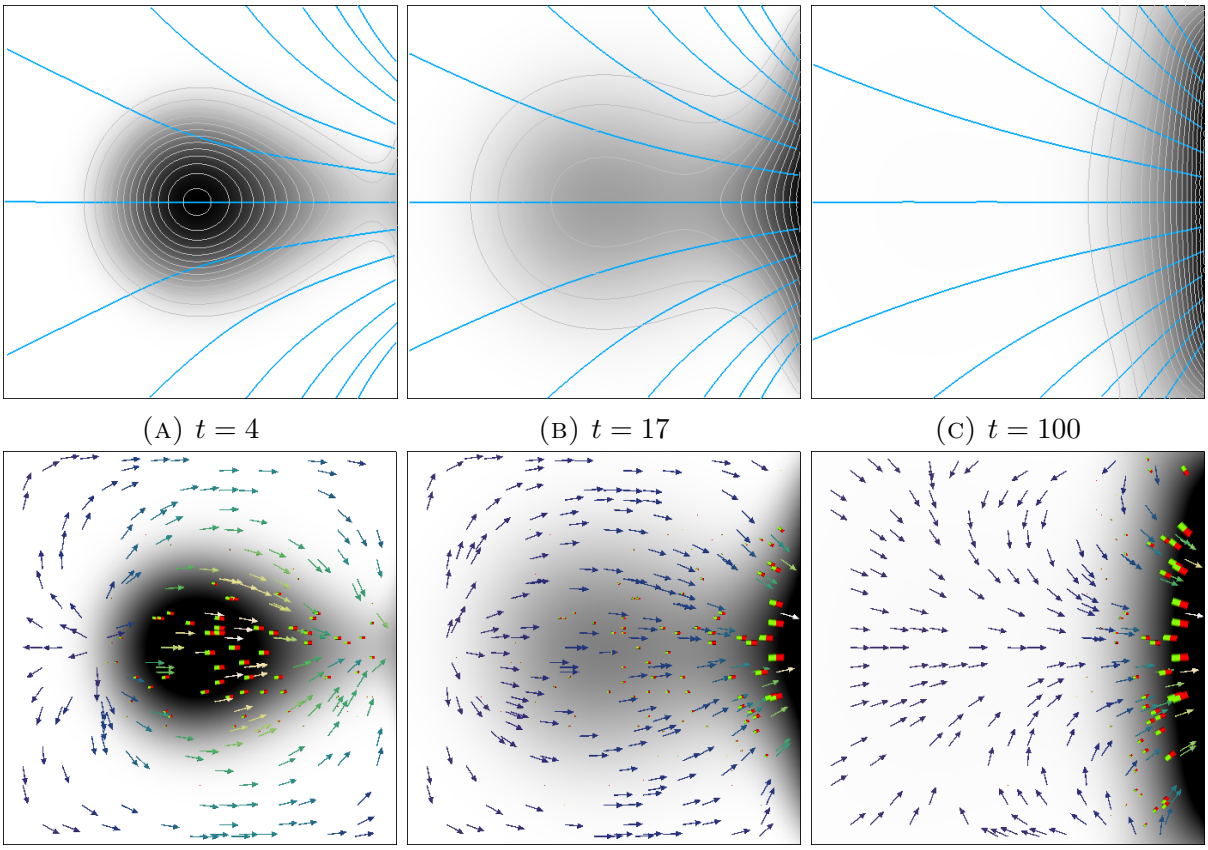

(A) $t = 4$ (B) $t = 17$ (C) $t = 100$

(D) $t = 4$ (E) $t = 17$ (F) $t = 100$

FIGURE 4.5. Particles density visualized by black color levels, where darker means higher density. Gray contour lines underline density contrasts and blue lines represent streamlines of $\mathbf{h}$. Normalized arrows indicate stray field $\mathbf{h}_d$, brighter color means stronger magnitude. Red/green cylinders visualize magnetization $\mathbf{m}$. Dipole at $\mathbf{x}_s = (1.75, 0.5)$ with intensity $C_s = 5$.

7. C. Amrouche, C. Bernardi, M. Dauge, and V. Girault, *Vector potentials in three-dimensional non-smooth domains*, Math. Methods Appl. Sci. **21** (1998), no. 9, 823–864.
8. M. Arroyo, N. Walani, A. Torres-Sánchez, and D. Kaurin, *Onsager's variational principle in soft matter: Introduction and application to the dynamics of adsorption of proteins onto fluid membranes*, pp. 287–332, Springer International Publishing, 2018.
9. A. Capella, C. Melcher, and F. Otto, *Wave-type dynamics in ferromagnetic thin films and the motion of Néel walls*, Nonlinearity **20** (2007), no. 11, 2519–2537.
10. R. Dautray, M. Artola, J. C. Amson, M. Cessenat, and J. L. Lions, *Mathematical analysis and numerical methods for science and technology: Volume 3 spectral theory and applications*, Mathematical Analysis and Numerical Methods for Science and Technology, Springer Berlin Heidelberg, 1990.
11. S. R. de Groot and P. Mazur, *Non-equilibrium thermodynamics*, Dover Books on Physics, Dover Publications, 1984.
12. P. Di Barba, A. Savini, and S. Wiak, *Field models in electricity and magnetism*, Springer Science & Business Media, 2008.
13. D. A. Di Pietro and A. Ern, *Discrete functional analysis tools for Discontinuous Galerkin methods with application to the incompressible Navier-Stokes equations*, Math. Comp. **79** (2010), 1303–1330.
14. ———, *Mathematical aspects of discontinuous galerkin methods*, Mathématiques et Applications, Springer Berlin Heidelberg, 2011.

15. C. Eck, M. Fontelos, G. Grün, F. Klingbeil, and O. Vantzos, *On a phase-field model for electrowetting*, Interfaces and Free Boundaries **11** (2009), no. 2, 259–290.
16. A. Einstein, *Über die von der molekularkinetischen Theorie der Wärme geforderte Bewegung von in ruhenden Flüssigkeiten suspendierten Teilchen*, Annalen der Physik **322** (1905), no. 8, 549–560.
17. L. Giacomelli and G. Grün, *Lower bounds on waiting time for degenerate parabolic equations and systems*, Interfaces and Free Boundaries **8** (2006), no. 1, 111–129.
18. V. Girault and P. A. Raviart, *Finite element methods for Navier-Stokes equations: Theory and algorithms*, Springer series in computational mathematics, Springer-Verlag, 1986.
19. D. Himmelsbach, M. Neuss-Radu, and N. Neuß, *Mathematical modelling and analysis of nanoparticle gradients induced by magnetic fields*, Journal of Mathematical Analysis and Applications **461** (2018), 1544–1560.
20. A. Hubert and R. Schäfer, *Magnetic domains: The analysis of magnetic microstructures*, Springer, 1998.
21. S. Kisseleff, R. Schober, and W. H. Gerstacker, *Magnetic nanoparticle based interface for molecular communication systems*, IEEE Communications Letters **21** (2017), no. 2, 258–261.
22. D. Kröner, *Numerical schemes for conservation laws*, Chichester ; New York : Wiley ; Stuttgart : Teubner, 1997.
23. M. Kruzik and A. Prohl, *Recent developments in the modeling, analysis, and numerics of ferromagnetism*, SIAM Review **48** (2006), 439–483.
24. J. E. Mayer and M. G. Mayer, *Statistical mechanics*, J. Wiley, 1940.
25. C. Melcher, *Thin-film limits for Landau-Lifshitz-Gilbert equations*, SIAM Journal on Mathematical Analysis **42** (2010), no. 1, 519–537.
26. ———, *Global solvability of the Cauchy problem for the Landau-Lifshitz-Gilbert equation in higher dimensions*, Indiana Univ. Math. J. **61** (2012), 1175–1200.
27. R. H. Nochetto, A. J. Salgado, and I. Tomas, *A diffuse interface model for two-phase ferrofluid flows*, Computer Methods in Applied Mechanics and Engineering **309** (2016), 497–531.
28. ———, *The equations of ferrohydrodynamics: Modeling and numerical methods*, Mathematical Models and Methods in Applied Sciences **26** (2016), no. 13, 2393–2449.
29. S. Odenbach, *Ferrofluids: Magnetically controllable fluids and their applications*, Lecture Notes in Physics, Springer Berlin Heidelberg, 2002.
30. L. Onsager, *Reciprocal relations in irreversible processes. i.*, Phys. Rev. **37** (1931), 405–426.
31. ———, *Reciprocal relations in irreversible processes. ii.*, Phys. Rev. **38** (1931), 2265–2279.
32. V. Polevikov and L. Tobiska, *On the solution of the steady-state diffusion problem for ferromagnetic particles in a magnetic fluid*, Mathematical Modelling and Analysis **13** (2008), no. 2, 233–240.
33. T. Qian, X. Wang, and P. Sheng, *A variational approach to moving contact line hydrodynamics*, Journal of Fluid Mechanics **564** (2006), 333–360.
34. R. E. Rosensweig, *Ferrohydrodynamics*, Dover Books on Physics, Dover Publications, 1997.
35. ———, *Basic equations for magnetic fluids with internal rotations*, Ferrofluids: Magnetically controllable fluids and their applications, Springer, 2002, pp. 61–84.
36. M. I. Shliomis, *Ferrohydrodynamics: Retrospective and issues*, Ferrofluids: Magnetically controllable fluids and their applications, Springer, 2002, pp. 85–111.
37. H. C. Torrey, *Bloch equations with diffusion terms*, Phys. Rev. **104** (1956), no. 3, 563–565.
38. H. Unterweger, J. Kirchner, W. Wicke, A. Ahmadzadeh, D. Ahmed, V. Jamali, C. Alexiou, G. Fischer, and R. Schober, *Experimental molecular communication testbed based on magnetic nanoparticles in duct flow*, IEEE Intern. Workshop on Signal Proc. Advances In Wireless Commun. (SPAWC) (2018), invited paper.
39. W. Wicke, A. Ahmadzadeh, V. Jamali, R. Schober, H. Unterweger, and C. Alexiou, *Molecular communication using magnetic nanoparticles*, IEEE Wireless Commun. Netw. Conf. (2018), 1–6.

(G. Grün) Friedrich-Alexander-Universität Erlangen-Nürnberg — Department of Mathematics — Cauerstrasse 11 — 91058 Erlangen — Germany
E-mail address: gruen@math.fau.de

(P. Weiß) Friedrich-Alexander-Universität Erlangen-Nürnberg — Department of Mathematics — Cauerstrasse 11 — 91058 Erlangen — Germany
E-mail address: patrick.weiss@math.fau.de